

Phototautomerization in pyrrolylphenylpyridine terphenyl systems

Nikola Basaric, Suma S Thomas, Vesna Blazek Bregovic, Nikola Cindro, and Cornelia Bohne

J. Org. Chem., **Just Accepted Manuscript** • Publication Date (Web): 30 Mar 2015

Downloaded from <http://pubs.acs.org> on March 31, 2015

Just Accepted

“Just Accepted” manuscripts have been peer-reviewed and accepted for publication. They are posted online prior to technical editing, formatting for publication and author proofing. The American Chemical Society provides “Just Accepted” as a free service to the research community to expedite the dissemination of scientific material as soon as possible after acceptance. “Just Accepted” manuscripts appear in full in PDF format accompanied by an HTML abstract. “Just Accepted” manuscripts have been fully peer reviewed, but should not be considered the official version of record. They are accessible to all readers and citable by the Digital Object Identifier (DOI®). “Just Accepted” is an optional service offered to authors. Therefore, the “Just Accepted” Web site may not include all articles that will be published in the journal. After a manuscript is technically edited and formatted, it will be removed from the “Just Accepted” Web site and published as an ASAP article. Note that technical editing may introduce minor changes to the manuscript text and/or graphics which could affect content, and all legal disclaimers and ethical guidelines that apply to the journal pertain. ACS cannot be held responsible for errors or consequences arising from the use of information contained in these “Just Accepted” manuscripts.



Phototautomerization in pyrrolylphenylpyridine terphenyl systems

Nikola Basarić,^{†*} Suma S. Thomas,[‡] Vesna Blažek Bregović,[†] Nikola Cindro,[†] and Cornelia

Bohne^{‡*}

[†] Department of Organic Chemistry and Biochemistry, Ruđer Bošković Institute, Bijenička cesta

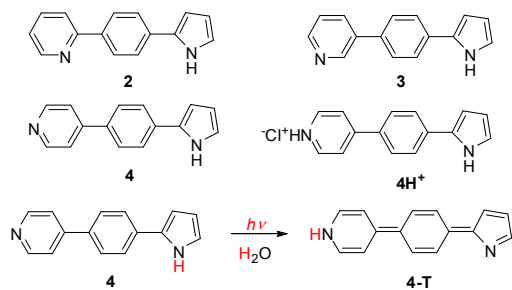
54, 10 000 Zagreb, Croatia. Fax: + 385 1 4680 195; Tel: +385 1 4561 141

[‡] Department of Chemistry, University of Victoria, Box 3065 STN CSC, Victoria BC, V8W

3V6, Canada. Fax:+ 250 721 7147; Tel:+ 250 721 7151

Corresponding authors' E-mail addresses: NB nbasarić@irb.hr; CB cornelia.bohne@gmail.com

Graphical abstract



Abstract: [4-(2-Pyrrolyl)phenyl]pyridines **2-4** were synthesized and their photophysical properties and reactivity in phototautomerization reactions investigated by fluorescence spectroscopy and laser flash photolysis (LFP). The pK_a for the protonation of the pyridine nitrogen in **2-4** was determined by UV-vis and fluorescence titration ($pK_a = 5.5$ for **4**). On excitation in polar protic solvents **2-4** populate charge transfer (CT) states leading to an enhanced

1
2
3 basicity of the pyridine ($pK_a^* \approx 12$) and enhanced acidity of pyrrole ($pK_a^* \approx 8-9$) enabling excited
4 state proton transfer (ESPT). ESPT gives rise to phototautomers and significantly quenches the
5 fluorescence of **2-4**. Phototautomers **2-T** and **4-T** were detected by LFP with strong transient
6 absorption maxima at 390 nm. Phototautomers **2-T** and **4-T** decayed by competing uni- and
7 bimolecular reactions. However, at pH 11 the decay of **4-T** followed exponential kinetics with a
8 rate constant of $4.2 \times 10^6 \text{ s}^{-1}$. The pyridinium salt **4H⁺** forms a stable complex with cucurbit[7]uril
9 (CB[7]) with 1:1 stoichiometry ($\beta_{11} = (1.0 \pm 0.2) \times 10^5 \text{ M}^{-1}$, $[\text{Na}^+] = 39 \text{ mM}$). Complexation to
10 CB[7] increased the pK_a for **4H⁺** ($pK_a = 6.9$) and changed its photochemical reactivity. Homolytic
11 cleavage of the pyrrole NH leads to the formation of an N-radical because of the decreased
12 acidity of the pyrrole in the inclusion complex.
13
14
15
16
17
18
19
20
21
22
23
24
25
26
27
28

29 **Key words:** excited state proton transfer (ESPT), pyridine, pyrrole, laser flash photolysis,
30 inclusion complexes, cucurbit[7]uril
31
32
33
34
35
36

37 Introduction

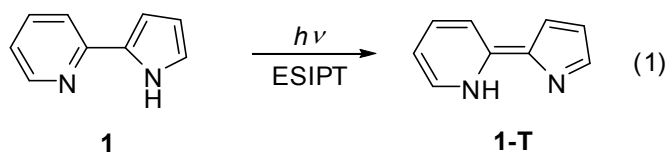
38 Proton transfer is a fundamental reaction in chemistry and biology¹ that has received much
39 attention due to fundamental aspects, as well as numerous applications.² Upon electronic
40 excitation, some organic functional groups exhibit enhanced acidity or basicity.^{3,4} If these sites
41 are in close proximity, excitation can lead to excited-state intramolecular proton transfer
42 (ESIPT).^{5,6,7,8} However, if the basic and acidic sites are not at a short distance, proton transfer
43 can be feasible either via double proton transfer or via a relay mechanism over bridges of protic
44 molecules.⁹ The latter process is particularly interesting in biological systems and involves
45 chains of polar amino acids and H₂O molecules,^{10,11,12} or coupled electron transfer and proton
46
47
48
49
50
51
52
53
54
55
56
57
58
59
60

transfer.^{13,14} Long-range proton transfer also takes place in respiratory complexes,¹⁵ whereas absorption of light in bacteriorhodopsin enables the function of a proton pump that moves protons through a membrane against a gradient.^{16,17} The mechanism of ESPT that involves solvent-relay shuffling of a proton has been documented for 7-azaindoles¹⁸ and 7-hydroxyquinoline,^{19,20,21,22,23} and has been used for the probing of structural dynamics in proteins.²⁴ Furthermore, proton transfer taking place via relay of H₂O-molecules has been used to study dynamics of membranes and micelles.^{25,26,27}

ESIPT in the pyrrolylpyridine systems has been well documented.²⁸ In these examples the pyrrole or indole NH is the acidic site, whereas the pyridine nitrogen is the basic site.^{29,30,31,32,33}

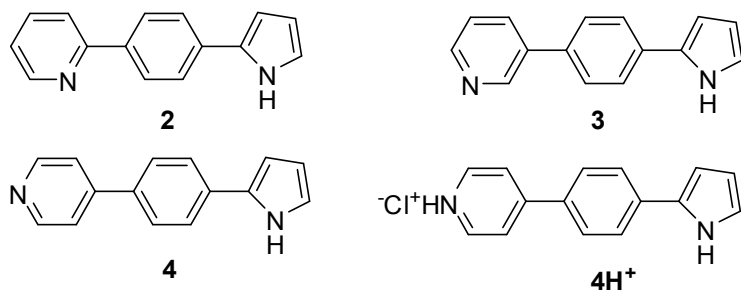
For example, photoexcitation of pyrrolylpyridine **1** in nonpolar solvents leads to ESIPT and to the population of phototautomer **1-T** (Eq. 1) which was detected by fluorescence spectroscopy.³¹

In the corresponding *meta* and *para* pyridine derivatives wherein the acidic and basic sites are distant, solvent-assisted double proton transfer occurs giving rise to phototautomers, or H-bonding complexes with the solvent are formed, leading to a de-excitation via an internal conversion channel.^{34,35,36}



Herein we report on the investigation of solvent-assisted phototautomerization (formal proton transfer) in a series of pyrrolylphenylpyridine terphenyl derivatives **2-4**. The photophysical properties of molecules **2-4** were investigated by fluorescence spectroscopy, whereas formation of the phototautomers was probed by laser flash photolysis (LFP). Furthermore, the complexation of **4H**⁺ with cucurbit[7]uril (CB[7]) was investigated, because inclusion complexes

with CB[n]s were shown to alter photochemical reactivity³⁷ and these complexes have been the focus of intensive research,³⁸ particularly owing to the potential applicability as drug delivery vehicles^{39,40,41} or photoswitches.^{42,43} Herein we demonstrate that complexation of 4H^+ with CB[7] changes its photochemical reactivity and prevents phototautomerization.

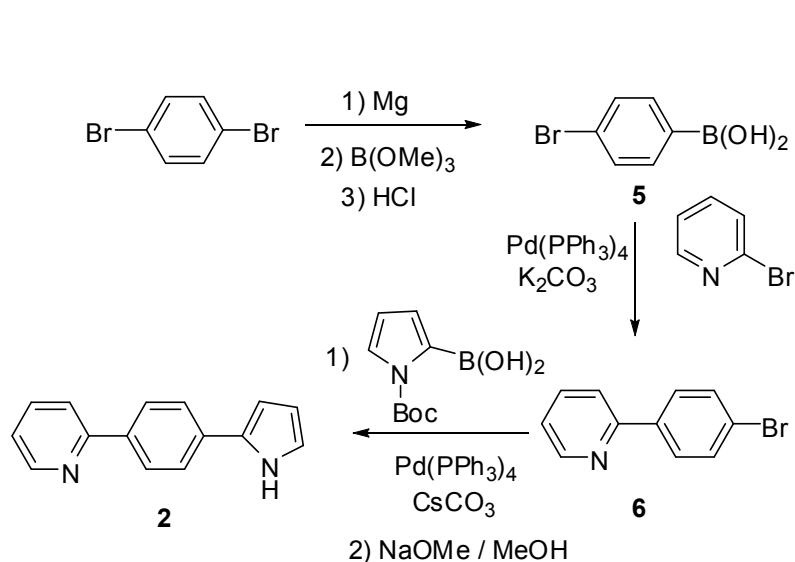


Results

Synthesis

Pyrrole derivatives **2-4** were prepared from the corresponding (4-bromophenyl)pyridines (Schemes 1-3). For the *ortho* derivative, 4-bromophenyl boronic acid (**5**) was prepared first, that in the Suzuki coupling with 2-bromopyridine afforded 2-(4-bromophenyl)pyridine (**6**)^{44,45} in the yield of 29%. The subsequent Suzuki reaction with the pyrrole boronic acid,⁴⁶ according to the optimized conditions for the arylation with pyrrole⁴⁷ and the Boc-deprotection in basic conditions (Scheme 1) gave the target compound **2**.⁴⁸

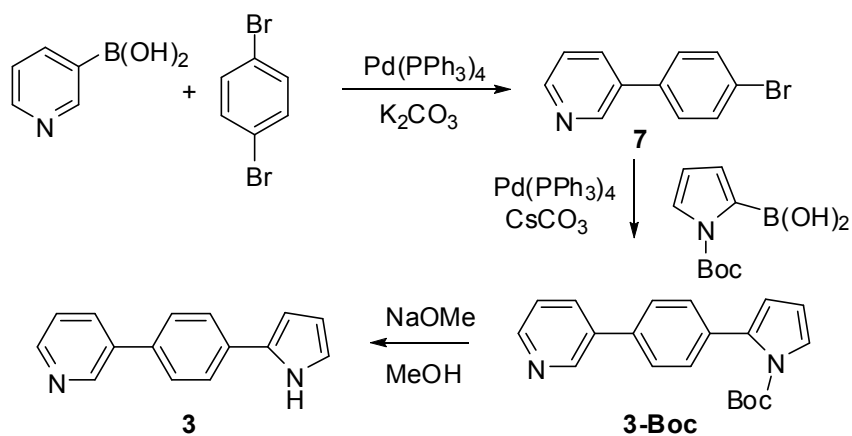
Scheme 1.



22
23
24
25
26
27
28
29
30
31
32
33

Synthesis of *meta* derivative **3** started from the commercially available 3-pyridine boronic acid that was arylated in a Suzuki coupling to afford bromide **7**,^{49,50} and subsequently in another Suzuki coupling with pyrrole boronic acid gave **3-Boc** derivative. Boc-deprotection in basic conditions gave the target compound in the overall yield of $\approx 20\%$ (Scheme 2).

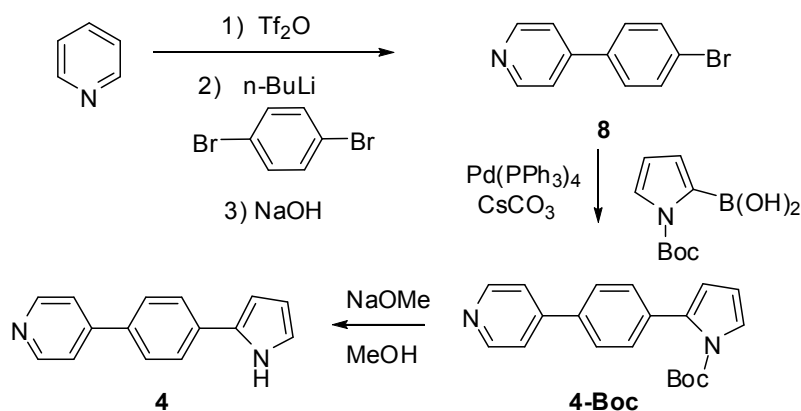
Scheme 2.



1
2
3
4
5
6
7
8
9
10
11
12
13
14
15
16
17
18
19
20
21
22
23
24
25
26
27
28
29
30
31
32
33
34
35
36
37
38
39
40
41
42
43
44
45
46
47
48
49
50
51
52
53
54
55
56
57
58
59
60

The synthetic strategy for *para*-derivative **4** was different than for **2** and **3** since bromide **8** was not prepared in a metal-catalyzed cross-coupling. Instead, according to a modification of the published procedure,⁵¹ pyridine was activated by transforming it to a triflate salt, which enabled nucleophilic addition of *p*-bromophenyllithium generated *in situ*. The reaction gave the 1,2- (minor) and 1,4-adducts (major) which were isolated as a mixture and without characterization treated with a base to afford **8**⁴⁸ as the major product, isolated in the overall yield of 25%. Subsequent arylation with pyrrole boronic acid, as for the *ortho* and *meta* derivative, and Boc-deprotection gave the target compound (Scheme 3).

Scheme 3.



Fluorescence measurements

Absorption spectra of **2-4** taken in CH_3CN (Fig. 1 top) exhibit an absorption band with a maximum at around 327 nm corresponding to the HOMO-LUMO transition and population of S_1 . The geometries of the two conformers of **4** and orbitals involved in the electronic transition are presented in the supporting information (Fig. S1 and S2, Tables S1, S3 and S4 in the SI). The

excitation has a significant charge transfer (CT) character, leading to an electron density enhancement on the pyridine and a decrease on the pyrrole.

Fluorescence spectra of **2-4** were measured in cyclohexane, CH₃CN and CH₃CN-H₂O (1:1, Fig. 1 bottom and Fig. S5-S12 in the SI). In cyclohexane, the fluorescence spectra of **2-4** are structured with a vibronic progression of 1400 cm⁻¹. The increase in solvent polarity shifts the maximum of the emission to longer wavelengths (Fig. 1 bottom, and Fig. S7, S9, S11 in the SI), and leads to a disruption of the vibronic structure. These findings suggest an increase of the dipole moment for the excited state, in agreement with the calculation for **4** (see Table S3 in the SI).

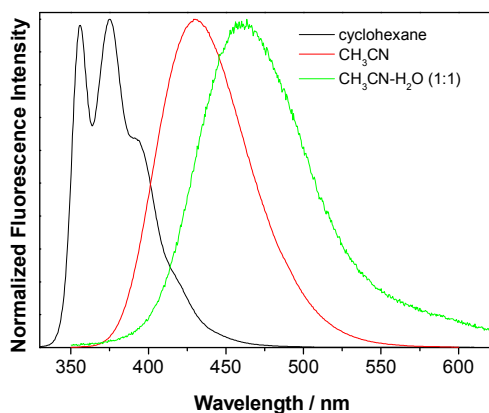
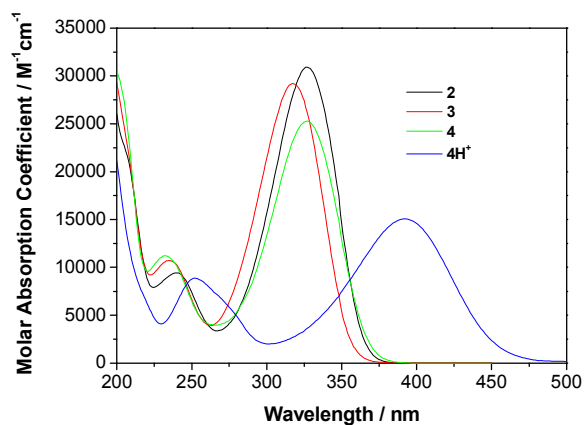


Fig 1. Absorption spectra of **2-4**, and **4H⁺** in CH₃CN (top), and normalized fluorescence spectra of **4** in different solvents (bottom).

Quantum yields of fluorescence for **2-4** were measured by use of quinine sulfate / 0.05 M H₂SO₄ as a reference (see equation S1 in the SI), whereas lifetimes were measured by time-correlated single photon counting (SPC). Similar quantum yields were measured for **2-4** in cyclohexane and CH₃CN (Table 1). The decays from S₁ for **2-4** were faster in cyclohexane than in CH₃CN, and in cyclohexane the kinetics were fit to a sum of two exponentials, while the kinetics was fit to a monoexponential function in CH₃CN (Table 1). Although straightforward assignment of decay components in cyclohexane is not possible at this point, the observation could be interpreted as due to locally excited (LE) and charge transfer (CT) states, or aggregation of molecules in that solvent. However, fine vibronic structure observed in the steady state spectra in cyclohexane does not suggest aggregation. Nevertheless, in CH₃CN only one S₁ state is populated with a significant CT character wherein the pyrrole moiety becomes relatively positively charged (and therefore, more acidic than in S₀) and the pyridine relatively negatively charged (more basic than in S₀).

Table 1. Photophysical properties of **2-4** and **4H⁺**

	Φ^a	τ^b	Φ^a	τ^b	Φ^a	τ^b
	(cyclo.)	(cyclo.)/ns	(CH ₃ CN)	(CH ₃ CN)/ns	(CH ₃ CN-H ₂ O)	(CH ₃ CN-H ₂ O)/ns
2	0.90±0.03	(60-120)×10 ⁻³	0.95 ± 0.05	2.14 ± 0.01	0.046 ± 0.003	(90-120)×10 ⁻³
		1.25±0.01				0.40 ± 0.05
3	0.90±0.02	(70-100)×10 ⁻³	0.83 ± 0.03	2.28 ± 0.01	(2.7 ± 0.2)×10 ⁻³	< 30×10 ⁻³
		1.25±0.01				

1						
2						
3	4	0.95±0.02	(60-100)×10 ⁻³	0.91 ± 0.03	2.29 ± 0.01	0.049 ± 0.003
4						(90-150)×10 ⁻³
5			1.41±0.01			0.3 ± 0.1
6						
7	4H⁺	-	-	0.012±0.002	0.11 ± 0.01	-
8						
9			^c		0.68 ± 0.02	
10						

^a Fluorescence quantum yields measured by use of quinine sulfate in 0.05 M H₂SO₄ as a reference ($\Phi_f = 0.53$).⁵² Errors correspond to averaged data measured at three different wavelengths.

^b Measured by SPC. Errors correspond to those obtained by global fitting of three decays at different emission wavelengths. The pre-exponential factors for the fastest lifetime of the non-exponential decays were: 0.03-0.05 in cyclohexane, 0.6-0.95 in CH₃CN-H₂O with a significant dependence on the emission wavelengths, and 0.4-0.5 for **4H⁺** in CH₃CN.

^c Estimated fluorescence quantum yield measured for the emission band at 570 nm by use of acridine yellow in CH₃OH as a reference ($\Phi_f = 0.57$).⁵³ Errors correspond to averaged data measured at three different wavelengths.

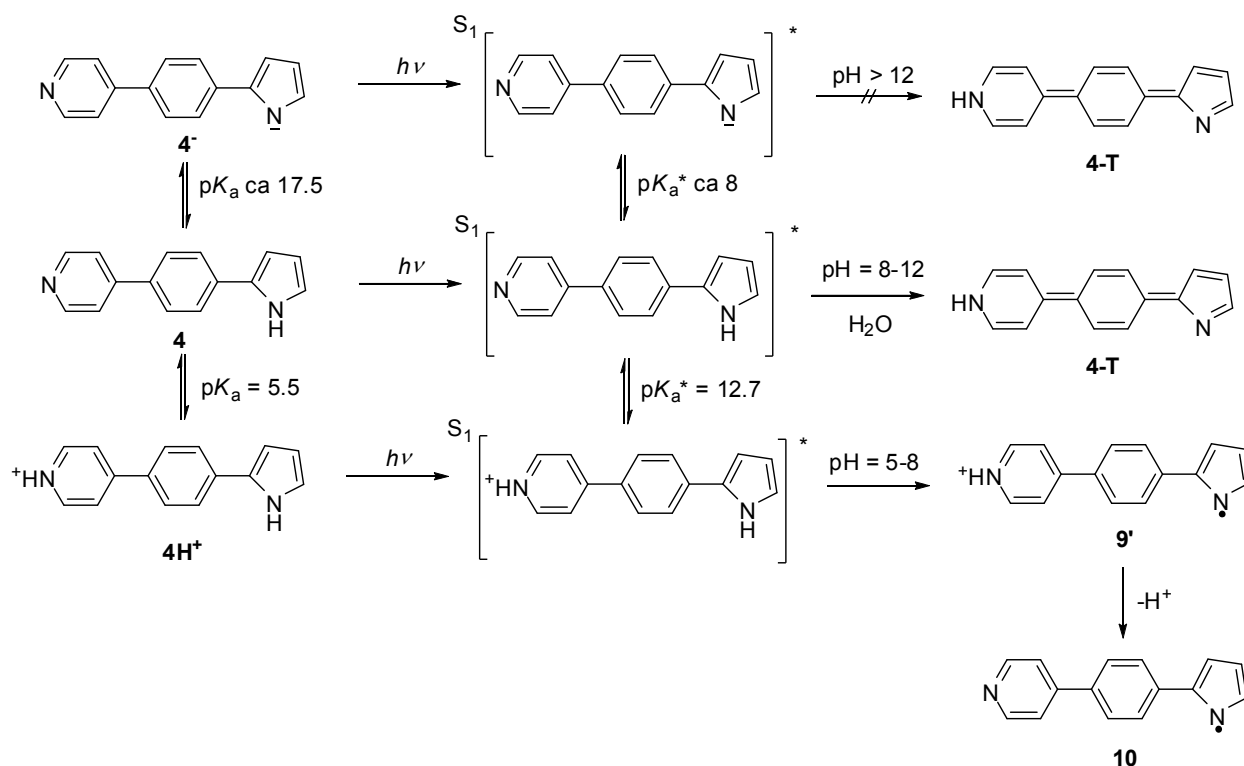
Protonation of the pyridine nitrogen in **4H⁺** significantly shifts the position of the absorption maximum bathochromically to 393 nm (Fig. 1, top) owing to a larger stabilization of S₁ than S₀ by protonation of **4**. However, dilution of the solution (from 5 × 10⁻⁵ M to 5 × 10⁻⁶ M) changes the appearance of the spectrum with the shift of the maximum to 327 nm (Fig. S13 in the SI). Although these spectral changes could be related to deaggregation of the molecules by dilution, the spectral changes are consistent with the deprotonation of **4H⁺** because the changes parallel those observed in the pH titration. Therefore, **4H⁺** in CH₃CN behaves as a weak acid suggesting that both **4** and **4H⁺** are present in solution.

1
2
3 Fluorescence spectra of 4H^+ in CH_3CN are also strongly dependent on concentration (Fig. S14 in
4 the SI) with two emission maxima at 430 and 570 nm, corresponding to **4** and 4H^+ , respectively.
5
6 Moreover, the fluorescence decay of 4H^+ in CH_3CN is bi-exponential, due the presence of **4** and
7
8 4H^+ . The fluorescence quantum yield of 4H^+ in CH_3CN ($c = 5 \times 10^{-6}$ M) measured for the
9
10 emission between 430 and 750 nm was estimated by exciting the sample at ca. 410 nm where
11
12 only 4H^+ absorbs, giving a value about 75 times lower than for **4**. Increase of temperature also
13
14 led to the deprotonation of 4H^+ , as indicated by the change of the relative intensities of the bands
15
16 at 430 nm and 570 nm (Fig. S15 in the SI). These fluorescence results are consistent with the
17
18 changes observed in the absorption spectra when the concentration of 4H^+ was altered.
19
20
21
22
23

24 Addition of a protic solvent (H_2O) to the CH_3CN solution strongly quenches the fluorescence of
25
26 **2-4**. This finding indicates that a protic solvent opens an efficient deactivation channel from S_1 .
27
28 As discussed above, **2-4** populate CT states in a polar solvent wherein the pyridine nitrogen
29
30 becomes more basic and the pyrrole more acidic. Therefore, quenching of fluorescence in the
31
32 presence of protic solvent can be rationalized by ESPT leading to the protonation of the pyridine
33
34 nitrogen and/or deprotonation of the pyrrole NH (Scheme 4). Furthermore, a new shoulder
35
36 appears ($\lambda > 550$ nm) in the fluorescence spectrum of **4** taken in $\text{CH}_3\text{CN-H}_2\text{O}$ (Fig. S5, S6, S11
37
38 and S12 in the SI) that is associated with the fluorescence of 4H^+ formed by ESPT (see below).
39
40
41
42
43
44
45
46
47
48
49
50
51
52
53
54
55
56
57
58
59
60

Decays of fluorescence of **2-4** in $\text{CH}_3\text{CN-H}_2\text{O}$ were multi-exponential, but due to the presence of
a very fast component, analysis of the decay components was not possible with the SPC
equipment used.

Scheme 4. Phototautomerization of **4** and formation of its radical in aqueous solution depending on pH.

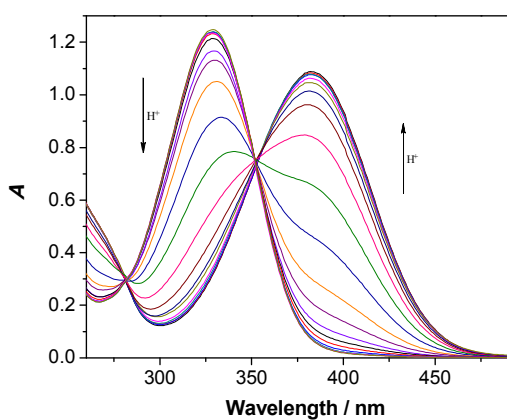


Acid-base properties were investigated for **2-4** by UV-vis and fluorescence titrations. For *para* derivative **4**, the pH titrations were performed in H₂O in the absence of a buffer, and in the presence of phosphate or citrate buffers at two different concentrations of **4**. The variation of pH in the range 3-7 induced UV-vis and fluorescence spectral changes (Fig. 2). These spectra were processed by multivariate nonlinear regression analysis using the SPECFIT software^{54,55,56} to reveal the pK_a of 5.5 ± 0.1 determined using different methods (Fig. S26-S37 and Table S9 in the SI). This value matches with the pK_a for the protonation of the pyridine nitrogen (pK_a = 5.2).⁵⁷ Similar spectral changes were observed in the UV-vis pH titrations of **2** and **3** (Figs S16, S17,

1
2
3
4
5
6
7
8
9
10
11
12
13
14
15
16
17
18
19
20
21
22
23
24
25
26
27
28
29
30
31
32
33
34
35
36
37
38
39
40
41
42
43
44
45
46
47
48
49
50
51
52
53
54
55
56
57
58
59
60

S22 and S23) which were processed by SPECFIT software to reveal the pK_a values of ≈ 4.8 (see Tables S7 and S8 in the SI).

The pK_a^* value for the protonation of the pyridine nitrogen in **4** in S_1 was estimated from the fluorescence titration by use of the Förster cycle.³ Nonlinear regression analysis of the fluorescence titration data revealed the position of the emission maxima in aqueous solution for **4** and $4H^+$ at 484 and 580 nm, respectively (Table S9 in the SI). These values correspond to the increase of basicity of the pyridine nitrogen on excitation to S_1 of $\Delta pK = 7.2 \pm 0.2$; that is, the estimated value of pK_a^* is 12.7 ± 0.2 . For **2** and **3** Förster cycle analysis could not be applied to determine pK_a^* for the protonation of pyridine since the corresponding protonated form $2H^+$ is not fluorescent, and due to generally very weak fluorescence of both **3** and $3H^+$ (see Figs S18-S21, S24 and S25 in the SI). In contrast to pyridine, pyrrole behaves as a weak acid. The reported pK_a value for deprotonation of pyrrole is 17.5.⁵⁷ Therefore, we could not determine the pK_a for the deprotonation of pyrrole for compound **4** in the aqueous solution.



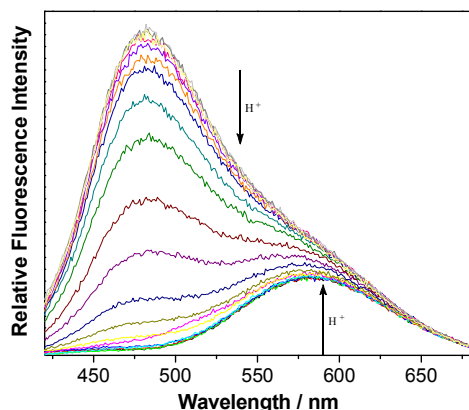


Fig. 2. UV-vis (top, $[4] = 5.3 \times 10^{-5}$ M) and fluorescence spectra (bottom, $\lambda_{\text{ex}} = 350$ nm, $[4] = 5.3 \times 10^{-6}$ M) at different pH values (from 3.0 to 7.5) in the presence of citrate buffer (0.05 M).

Inclusion complex with cucurbit[7]uril (CB[7])

Positively charged 4H^+ is a good candidate to form a host-guest complex with CB[7]. This macrocyclic host is known to bind well guests with positive charges and hydrophobic moieties,⁴² where the hydrophobic moiety fits within the cavity of the CB[n] and the positive charge is stabilized by interaction with the carbonyl groups. The association equilibrium constant was determined by UV-vis titration. To assure that the solution contained only 4H^+ , the titration was performed at pH 3.5 in the presence of citrate buffer. Addition of CB[7] induced a hypochromic and very weak bathochromic shift indicative of complex formation (Fig. 3). An overall binding model with the formation of a 1:1 complex between 4H^+ and CB[7] was employed (see the SI, page S29) where the binding of sodium cations (39 mM) to CB[7] was not accounted for in separate equilibria. The overall binding constant⁵⁸ β_{11} of $(1.0 \pm 0.2) \times 10^5 \text{ M}^{-1}$ was determined from two independent experiments for the absorption change at 360, 380 and 390 nm (Fig. S38-S39 and Table S11 in the SI).

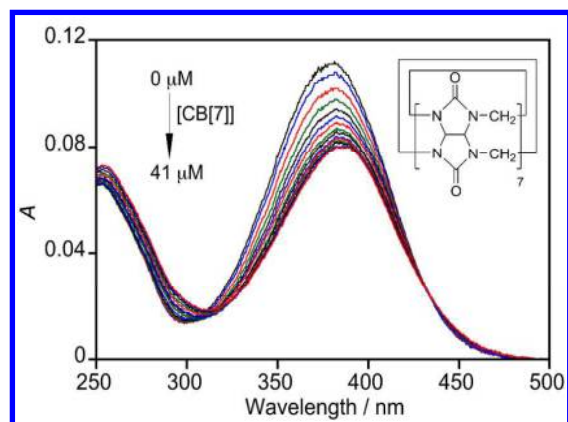
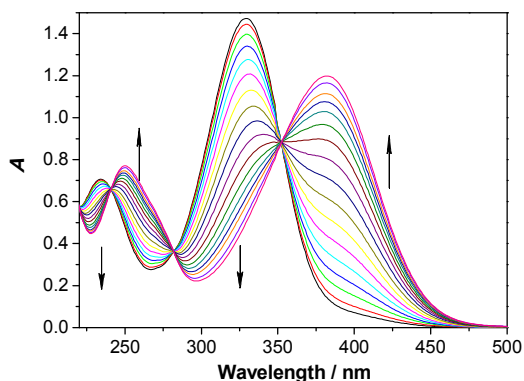


Fig 3. Absorption spectra for 4H^+ ($5\ \mu\text{M}$) in citrate buffer ($47\ \text{mM}$, $\text{pH} = 3.5$, $[\text{Na}^+] 39\ \text{mM}$) in the absence and presence of different concentrations of CB[7].

Complexation with CB[n] changes the $\text{p}K_{\text{a}}$ of bound guest molecules,^{59,60} and therefore influences ES IPT reactivity of complexed guests.⁶¹ This variation of $\text{p}K_{\text{a}}$ upon complexation was used for logic gates⁶² or drug delivery systems.^{63,64,65} Therefore, we investigated the use of CB[n] to modulate the $\text{p}K_{\text{a}}$ of **4** by performing titrations with CB[7] in non-buffered solution wherein the formation of the inclusion complex is anticipated to lead to the pyridine protonation. In the titration experiment, an aqueous solution of CB[7] containing $100\ \text{mM}$ NaCl was added to solutions of **4** in $\text{CH}_3\text{CN}-\text{H}_2\text{O}$ (1:9 or 1:99, both containing $100\ \text{mM}$ NaCl). The band at $330\ \text{nm}$ disappeared with concomitant formation of a new band at $390\ \text{nm}$ (Fig. 4 and Fig. S40 in the SI). The titration data resemble the ones seen in the pH titration (Fig. 2 top), where the absorption with maximum at $390\ \text{nm}$ corresponds to 4H^+ . This finding indicates that CB[7] enhances the basicity of **4**, leading to a stabilization of 4H^+ in the inclusion complex.

To determine the $\text{p}K_{\text{a}}$ of 4H^+ in the CB[7] complex we performed a pH titration of **4** in the presence of a large excess of CB[7] ($0.5\ \text{mM}$) to ensure that all **4** is bound to the complex, since it is known that the neutral form of guests have a lower stability constants than the cationic forms.^{38,42,43} The resulting UV-vis spectra (Fig. S41 in the SI) were processed by multivariate

1
2
3 nonlinear regression analysis using the SPECFIT program^{54,55,56} to reveal the pK_a value of $6.97 \pm$
4
5
6 0.05. The higher pK_a value ($\Delta pK_a \approx 1.5$) is in accordance with the precedent literature.^{59,60}
7
8
9

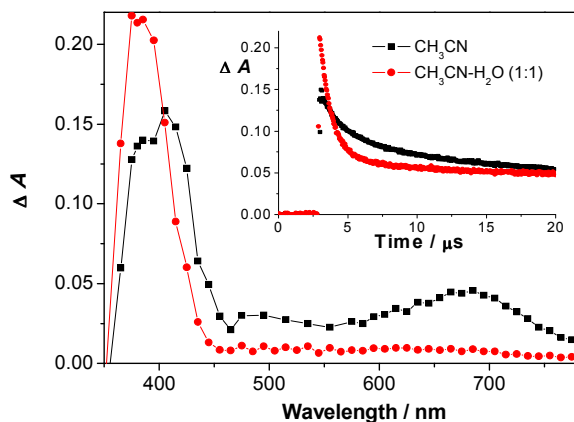


10
11
12
13
14
15
16
17
18
19
20
21
22
23
24 Fig. 4. Absorption spectra for the titration of **4** (5×10^{-5} M in $\text{CH}_3\text{CN-H}_2\text{O}$ 1:10, 100 mM NaCl)
25
26 with CB[7] (1 mM in H_2O , 100 mM NaCl, CB[7] = 0.6×10^{-5} M) in the absence of buffer. The
27
28 curves were corrected for dilution.
29
30
31
32

33 Laser Flash Photolysis (LFP)

34
35 LFP measurements for solutions in CH_3CN and $\text{CH}_3\text{CN-H}_2\text{O}$ were performed for isomers **2-4**, as
36
37 well as for the salt of 4H^+ to probe for the formation of phototautomers by ESPT. No
38
39 phototautomers are expected to be formed in CH_3CN . Transient absorption spectra for isomers **2-**
40
41 **4** in CH_3CN showed an absorption band with a maximum at 410 nm, and a weaker band at 680
42
43 nm (Fig. 5). Addition of H_2O to the CH_3CN solution significantly changed the appearance of the
44
45 transient absorption (Fig. 5 and Fig S42 in the SI). The results in CH_3CN (Fig. 5, black lines)
46
47
48 will be described first where for **2**, **3** and **4** the same transients were observed (Fig. S43-S49 in
49
50 the SI). These were assigned to radical-cations (**9**), which absorb at 680 nm, and pyrrolyl N-
51
52 centered (**10**) radicals, which absorb at 410 nm (Scheme 5) according to the comparison with
53
54
55
56
57
58
59
60

published transient spectra for phenylpyrroles⁶⁶ and indoles.^{67,68} The decay of the transient absorption measured in CH₃CN was fit to a sum of two exponentials ($k \approx 9 \times 10^5 \text{ s}^{-1}$ and $1 \times 10^5 \text{ s}^{-1}$ for **2**, $1 \times 10^6 \text{ s}^{-1}$ and $1 \times 10^5 \text{ s}^{-1}$ for **3**, and $3 \times 10^5 \text{ s}^{-1}$ and $\approx 10^4 \text{ s}^{-1}$ for **4**). The lifetimes were not affected by O₂, in agreement with a previous report that O₂ does not quench N-centered radicals⁶⁹ and radical-cations.^{66,67,68,69} Short-lived **9** absorbing in the visible part of the spectrum, and long-lived **10** absorbing at shorter wavelengths (380-420 nm), are probably formed in parallel processes. However, the observation of a growth kinetics with small amplitude in the transient absorption at $\approx 420 \text{ nm}$ (Fig. S48 in the SI) suggested that sequential formation of **9** and decay of this transient leading to the longer lived **10** may also take place. Since the absorption of solvated electron was not detected, an electron acceptor in the formation of **9** could have been H· radicals which are produced in the parallel process, traces of O₂ or H₂O molecules, or **2-4** in S₀ (less likely since radical-anions of **2-4** were not detected). Furthermore, in the homolytic cleavage of the pyrrole N-H bond and formation of **10**, H-acceptors could have been **2-4** in S₀, CH₃CN or O₂-molecules.



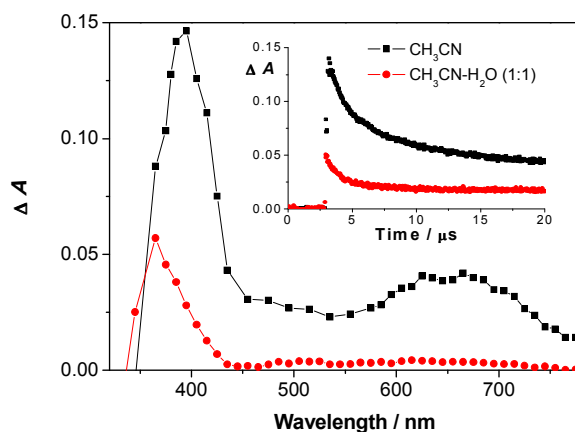
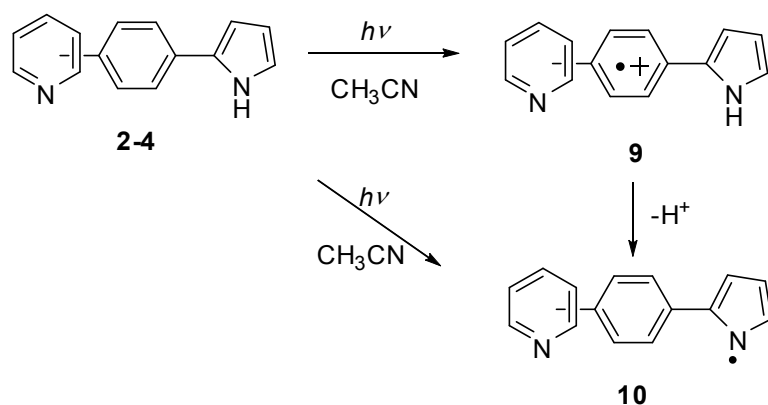


Fig. 5. Transient absorption spectra in O_2 purged and optically matched ($A_{355} \approx 0.35$) solutions for **2** (top) in CH_3CN (delay = 500 ns) and in CH_3CN-H_2O (delay = 200 ns); the inset shows the decays at 380 nm. Transient absorption spectra in O_2 purged and optically matched ($A_{355} \approx 0.32$) solutions for **3** (bottom) in CH_3CN (delay = 600 ns) and CH_3CN-H_2O (delay = 200 ns); the inset shows the decays at 380 nm.

Scheme 5. Photochemistry of **2-4** in aprotic solvent.



In CH_3CN-H_2O solution for **2-4** the transient absorption band in the visible region was not detected (Fig. 5, Fig. S43-S47 and S49 in the SI), in accordance with the assignment of the

1
2
3 transient observed in CH₃CN to radical-cations, which in aqueous solution rapidly decay by
4
5 proton transfer giving pyrrolyl radicals. Therefore, transients **9** are not observed when water is
6
7 present but the absorption for transient **10** is present (vide infra for discussion on lifetimes). In
8
9 the case of derivatives **2** and **4**, but not **3**, a new transient with absorption between 380 and 420
10
11 nm (Fig. 5, Fig. S42-S47 and S49 in the SI) was observed that is assigned to phototautomers **2-T**
12
13 (vide infra, scheme 7) and **4-T** (Scheme 4) formed by ESPT. These species gave rise to a higher
14
15 intensity of the transient absorbance at 380-420 nm, compared to the spectra in CH₃CN solutions
16
17 when the absorbance values at the excitation wavelengths were matched (Fig. 5 top). In the case
18
19 of **3**, analysis of the kinetics (vide infra) showed that **3-T** was not observed on the nanosecond
20
21 time scale (Fig. S42, S45 and S46 in the SI). Therefore, the spectrum in CH₃CN-H₂O (Fig. 5
22
23 bottom) corresponds only to intermediate **10**.
24
25
26
27
28

29 The relative contribution of the species in the photochemistry of **2-4** (Scheme 4) is expected to
30
31 be pH dependent for reactions in CH₃CN-H₂O because the formation of phototautomers is pH
32
33 dependent. At pH 11 (Fig. 6), the decay of the transient absorption was fit to a single-exponential
34
35 function ($4.1 \times 10^6 \text{ s}^{-1}$, $\tau = 240 \text{ ns}$) and was assigned to phototautomer **4-T** that at this pH decays
36
37 through a unimolecular process. A small off-set was observed at longer times which suggests
38
39 that a long-lived transient was present. This transient was more prominent at lower pHs and
40
41 corresponds to **10** (vide infra).
42
43
44
45

46 Decrease of the pH from 11 to 9-10 led to slower kinetics and the decay could not be fit to a
47
48 mono-exponential function. As will be shown below the kinetics correspond to a combination of
49
50 bimolecular and unimolecular processes, where the bimolecular process is assigned to the
51
52 reaction between two molecules of **4-T** which competes with the unimolecular decay of **4-T**. The
53
54 bimolecular component only becomes apparent when the unimolecular decay of **4-T** becomes
55
56
57
58
59
60

1
2
3 slower at these lower pH values. The contribution of the bimolecular process was minimized by
4 decreasing the energy of the laser pulse and the decay was fit by starting the fits at successively
5 longer delay times after the laser pulse until the kinetics fit to a monoexponential function (eq.
6 S3-S4 and Fig. S50 in the SI). The lifetime for the unimolecular decays of **4-T** were $\approx 2 \mu\text{s}$ at pH
7 10, and $4 \mu\text{s}$ at pH 9. A lengthening of the lifetime of **4-T** is expected since **4-T** undergoes base
8 catalysis to recover **4**. In addition to the decay of **4-T**, another transient was observed that
9 decayed over a much longer time window. This longer decay was fit to a monoexponential
10 function and had a lifetime of $120 \mu\text{s}$ ($k = 8.3 \times 10^3 \text{ s}^{-1}$). This transient is assigned to **10** based on
11 precedent in the literature.^{66,67,68,69}

12
13 On decrease of the pH below 8-9, the characteristic strong signal assigned to **4-T** disappeared.
14
15 Thus, in neutral and acidic solution only the longer-lived transient species was detected assigned
16 to radical **10**, decaying through a unimolecular process ($k = 8.3 \times 10^3 \text{ s}^{-1}$, $\tau = 120 \mu\text{s}$). However,
17 between pH values of 3 and 8 a new transient is observed (Fig. S51 in the SI). The lifetime for
18 this transient was estimated to be shorter than 100 ns, where this decay occurs over a short time
19 window and levels off before the long-lived decay occurs. Since the short-lived transient was not
20 detected in the visible part of the spectrum (at 680 nm), it cannot correspond to radical-cation **9'**.
21 According to the observation of the transient only at pH 3-8, its short lifetime and the absorption
22 at 390 nm, it may be related to the equilibrium between **4** and **4H⁺** in the ground state (Scheme
23 4). Upon excitation, singlet excited state **4** is protonated leading to **4H⁺** because of the higher
24 basicity in S_1 . Therefore this transient, was tentatively assigned to an excess of **4H⁺** in S_0 which
25 then decays to re-establish the ground-state equilibrium between **4** and **4H⁺**.
26
27
28
29
30
31
32
33
34
35
36
37
38
39
40
41
42
43
44
45
46
47
48
49
50
51
52
53
54
55
56
57
58
59
60

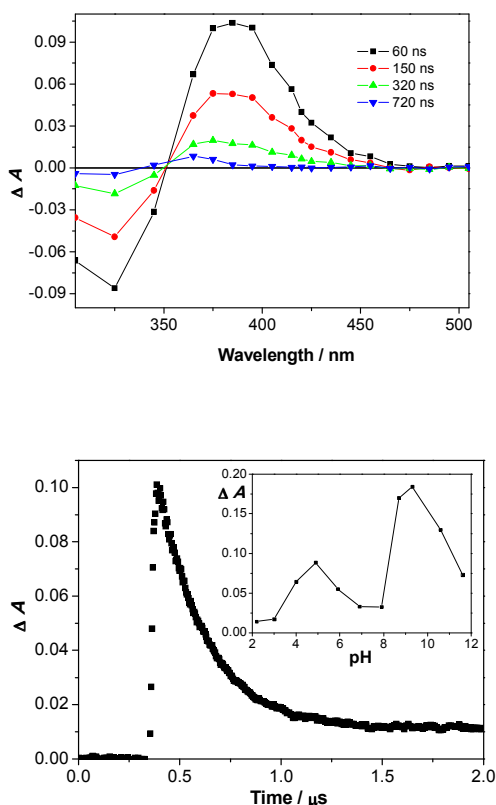


Fig. 6. Transient absorption spectra of **4** (top) in CH₃CN-H₂O (5:95), and decay at 380 nm at pH = 11. The inset shows the pH dependence of the transient absorbance intensity at 390 nm, right after laser excitation).

Formation of **4-T** by ESPT can only be facilitated in the pH range between the pK_a^* values for the pyridine protonation and the pyrrole deprotonation. These pK_a^* values were estimated in LFP experiments from the dependence of the initial transient absorption intensity right after the laser pulse collected at different pH values (Fig. 6 bottom, inset). Although this value is related to the formation of all transients, significantly stronger signal intensities were observed in the pH region between 9 and 12 where the characteristic transient assigned to **4-T** was detected. Thus, the estimated pK_a^* from the LFP experiment for the pyrrole deprotonation in S₁ is in the range of

1
2
3 8-9, and for the protonation of the pyridine this range is between 11 and 12 (Scheme 4). The
4
5 value for the pyridine pK_a^* in S_1 for $4H^+$ obtained by LFP (11-12) is somewhat lower than the
6
7 value obtained by Förster cycle analysis (12.7). However, it should be noted that the
8
9 determination of pK_a^* by Förster cycle is usually inaccurate.³ Irrespective of the accuracy for the
10
11 pK_a^* values, LFP measurements clearly showed that the formation and decay kinetics of
12
13 phototautomer **4-T** in aqueous solution is pH dependent.
14
15

16
17 In some ESPT systems double proton transfer takes place through a bimolecular reaction
18
19 involving two phototautomers, leading to non-exponential decays for the phototautomers.⁹
20
21 Therefore, the origin of the non-exponential decays for **2-T** and **4-T** was investigated using LFP
22
23 by changing the energy of the laser pulses. For competitive uni- and bimolecular reactions, the
24
25 decrease of the laser pulse energy leads to a decreased contribution of the bimolecular reaction to
26
27 the observed kinetics, because the bimolecular reaction depends on the concentration of
28
29 phototautomer, whereas unimolecular reactions are independent of the concentrations of
30
31 reactants. The contribution of the bimolecular reaction appears as an initial non-linear decay in
32
33 the semi-log plot of the kinetics (Fig. 7). Fourfold decrease of the laser pulse energy decreased
34
35 the amplitude of the bimolecular contribution of the decay. This finding indicates that only one
36
37 species is detected decaying by competing uni- and bimolecular reactions. Similar findings have
38
39 already been reported in the photochemistry of pyridylphenols.⁷⁰
40
41
42
43
44
45
46
47
48
49
50
51
52
53
54
55
56
57
58
59
60

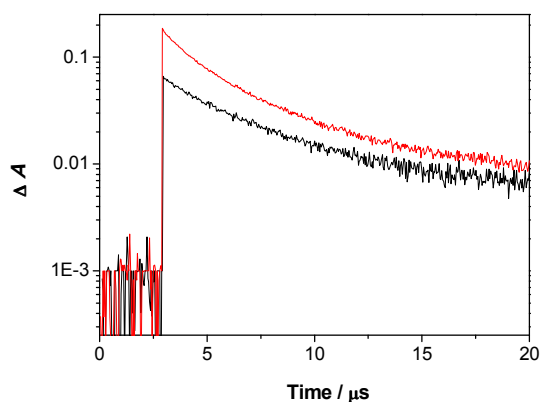


Fig. 7. Decay of the log of the transient absorbance at 400 nm for the solution of **4** in $\text{CH}_3\text{CN-H}_2\text{O}$ as a function of the relative laser pulse energy, estimated from the intensity of the benzophenone triplet at 525 nm (black line $\Delta A_{525} = 0.08$; red line $\Delta A_{525} = 0.31$) for optically matched solutions at the excitation wavelength ($A_{355} = 0.31$).

Proton transfer processes are usually characterized by a large primary isotope effect.⁷¹ To verify the assignment of the transient absorption to **2-T** and **4-T** we conducted LFP measurements for **2** and **4** in optically matched $\text{CH}_3\text{CN-H}_2\text{O}$ and $\text{CH}_3\text{CN-D}_2\text{O}$ solutions (Fig. 8 and Fig. S52 in the SI). Change of H_2O to D_2O resulted in weaker signal intensities and longer decay times for both compounds. From the ratio of the transient absorbance intensity immediately after the laser pulse the estimate for the isotope effect for the formation of tautomers is in the range 1.3.-2.5. However, the precise values of the isotope effects for the decay of transients was not warranted due to complex decay kinetics imposed by competing uni- and bimolecular reactions. The observed changes in the decay kinetics and the intensity of the transient absorption are due to the primary deuterium isotope effect for the formation and the decay of the transient species. These

1
2
3
4
5
6
7
8
9
10
11
12
13
14
15
16
17
18
19
20
21
22
23
24
25
26
27
28
29
30
31
32
33
34
35
36
37
38
39
40
41
42
43
44
45
46
47
48
49
50
51
52
53
54
55
56
57
58
59
60

results strongly indicate that the observed transient absorption corresponds to species formed by ESPT.

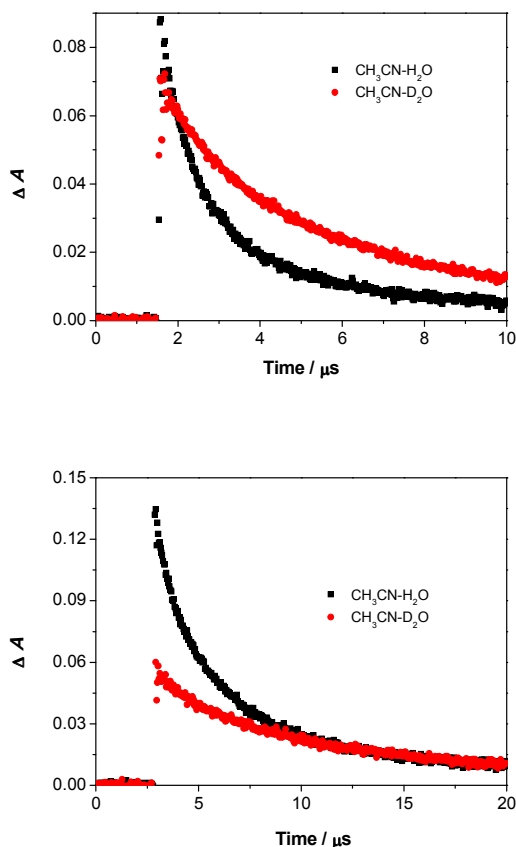
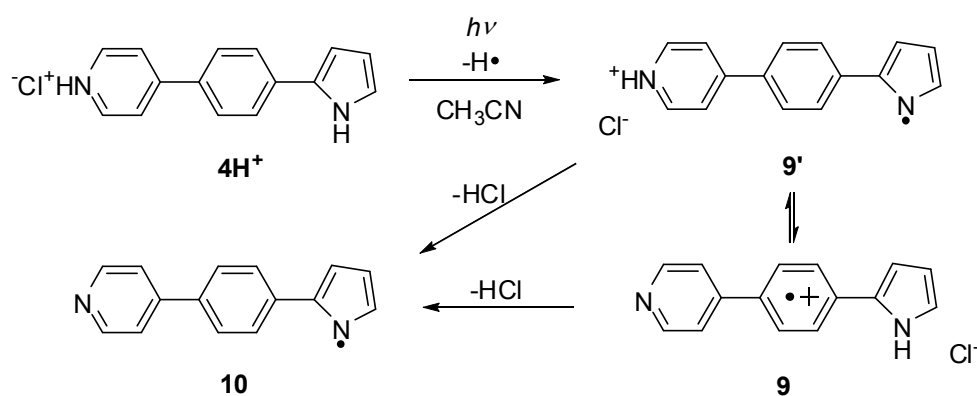


Fig. 8. Decay of transient absorbance at 420 nm in $\text{CH}_3\text{CN-H}_2\text{O}$ (1:1) and $\text{CH}_3\text{CN-D}_2\text{O}$ (1:1) for **2** (top) and **4** (bottom).

LFP measurements were also conducted for the salt of 4H^+ in CH_3CN and $\text{CH}_3\text{CN-H}_2\text{O}$ (Fig. S53-S56 and S57 left). In CH_3CN relatively weak transient absorption was observed with a maximum at 650 nm. The decay was fit to a sum of two exponentials with rate constants of 5×10^6 and $2 \times 10^4 \text{ s}^{-1}$. Due to the similarity of the transient absorption with radical-cation **9** the fast component was tentatively assigned to tautomeric radical-cation **9'** formed by homolytic N-H

1
2
3 cleavage of 4H^+ , whereas the slow component was assigned to radical **10** (Scheme 6). The
4
5 measurement in $\text{CH}_3\text{CN-H}_2\text{O}$ performed at neutral or slightly basic conditions gave rise to the
6
7 same transients as observed by LFP of **4** since 4H^+ at $\text{pH} > 5.5$ dissociates. Measurements in the
8
9 acidic solutions (H_2SO_4 , $\text{pH} 2$) gave rise to a transient absorption with a maximum at 370 nm and
10
11 weaker signals at 390 and 420-500 nm decaying with a rate constant of $4 \times 10^4 \text{ s}^{-1}$ that in analogy
12
13 was assigned to radical **10** (Fig S56 in the SI).
14
15
16
17
18
19

20 Scheme 6. Homolytic cleavage of 4H^+ observed in aprotic solvent.



LFP experiments were conducted with the $4\text{H}^+\cdot\text{CB}[7]$ complex to probe if the phototautomerization can take place within the cavity of $\text{CB}[7]$. Interestingly, the complexation with $\text{CB}[7]$ completely changed the photochemistry of 4H^+ . The signals corresponding to the phototautomer **4-T** were not detected. Instead, the transient absorption showed a maximum at 370 nm and a weaker broad band at 500-700 nm, similar to the transients observed in neat CH_3CN after decay of the radical-cation (Fig. 9 and Fig. S58 in the SI). Therefore we assigned the observed transient absorption in the presence of $\text{CB}[7]$ to the pyrrolyl radical **10**.

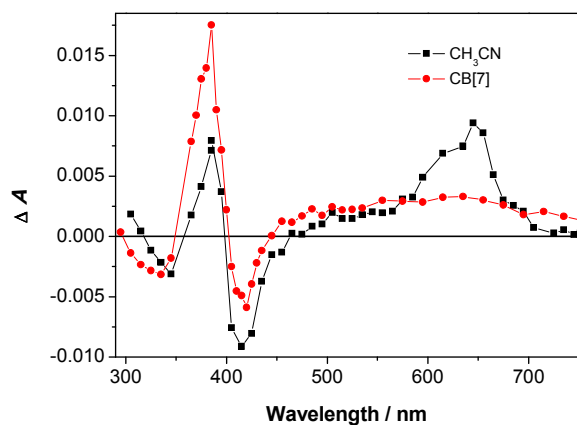


Fig. 9. Transient absorption spectra of 4H^+ (4.8×10^{-5} M) in CH_3CN and in aqueous NaCl in the presence of $\text{CB}[7]$ (2×10^{-4} M) taken 700 ns after the laser pulse. The solutions were optically matched ($A_{355} = 0.35$).

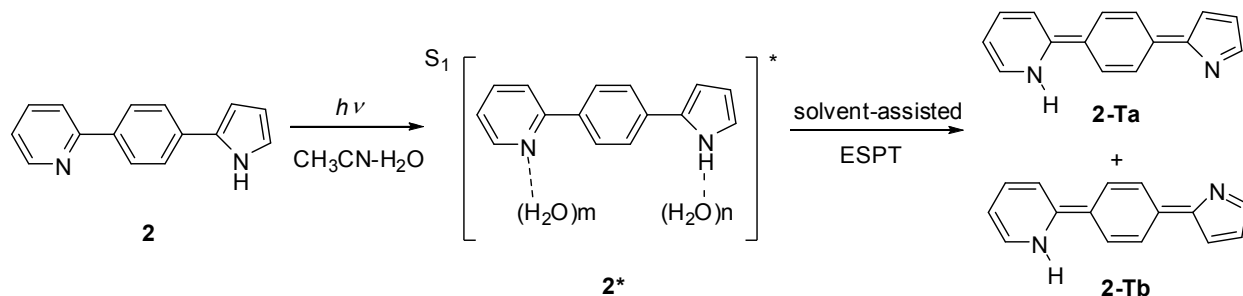
Discussion

Irradiation of **2-4** does not yield any stable photoproduct. However, quenching of fluorescence in aqueous solutions and LFP measurements indicate that ESPT takes place in H_2O leading to the formation of phototautomers. Since the acidic site (pyrrole) and the basic site (pyridine) are not in proximity, a polar protic solvent is essential to stabilize the CT-character of the S_1 state, and even more important, to act as a proton donor (acid) and acceptor (base).

Formation of phototautomer **2-T** from the *ortho* derivative in aqueous solution was assigned to the transient absorption with maximum at 390 nm. In near-neutral solution the decay for **2-T** was not exponential due to competing uni- and bimolecular reactions, as indicated by the dependence of the kinetics on the laser pulse energy. Only an estimate was possible for the decay time of **2-T**, $\tau \approx 1.5 \mu\text{s}$. The assignment of the transient to **2-T** was corroborated by a primary isotope

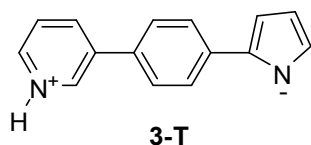
effect in D₂O solutions for its formation and decay (Fig 8). Moreover, **2-T** can in principle exist in two isomeric forms (**2-Ta** and **2-Tb**, Scheme 7). The observed non-exponential decay of **2-T** could in principle originate from the presence of these two isomers that undergo photochemical *E-Z* isomerization, and are characterized by different decay rate constants. However, the photochemical *E-Z*-isomerization would require a second photon. Furthermore, we observe similar non-exponential decay kinetics for **4-T** which cannot have two stereoisomers. Since the fast decay depends largely on the laser pulse energy, this kinetics is more likely due to the bimolecular reaction of **2-T** involving two proton transfers.

Scheme 7. Phototautomerization of **2**.



Meta derivative **3** also bears the basic pyridine nitrogen and the acidic pyrrole NH. Strong quenching of fluorescence in aqueous solution strongly indicates deactivation from S₁ by ESPT. Contrary to the transient spectra of **2**, the LFP for the *meta* isomer **3** did not give rise to a characteristic transient absorption that could be assigned to the phototautomer (Fig. S42 in the SI). Instead, in aqueous solution the transient absorption spectrum was narrower (370-390 nm), and the kinetics was slower than for **2-T**, that is the fast decay was missing. The spectrum for the photolysis of **3** was assigned to pyrrolyl radical **10** (Fig. 5 bottom). We do not have data for the

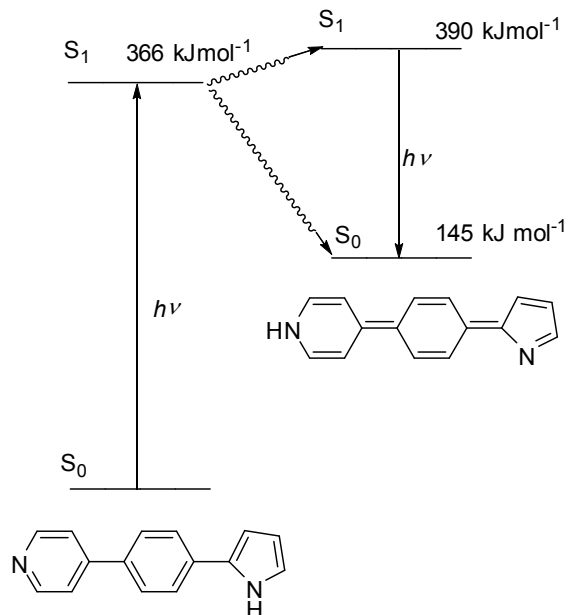
1
2
3 acidity/basicity of **3** in S_1 or spectroscopic evidence for the formation of the corresponding
4 phototautomer **3-T**. Nevertheless, **3-T** is a zwitterion that cannot be represented by a Kekulé
5 structure. Therefore, if this transient was formed in aqueous solution it would probably be very
6 short-lived (probably in the picosecond time-scale) and could not be detected by nanosecond
7 LFP. However, structurally related more stable zwitterions formed in photodehydration of
8 phenols have been reported and characterized by LFP.⁷² The other plausible explanation for the
9 observed quenching of fluorescence of **3** in aqueous solution does not involve ESPT and
10 formation of phototautomer **3-T**. Quenching may occur due to H-bonding with the solvent,
11 leading to a de-excitation via an internal conversion channel.^{34,35,36}
12
13
14
15
16
17
18
19
20
21
22
23
24
25
26



Excitation of **4** to S_1 leads to a significant enhancement of the pyridine basicity ($pK_a^* \approx 12$), as indicated by fluorescence measurements. In addition, concomitant enhancement of the pyrrole acidity in aqueous solution leads to ESPT and formation of phototautomer **4-T**, providing that the solution pH is in the range between the pK_a^* of pyrrole ($pH \approx 8-9$), and the pK_a^* of pyridine ($pH \approx 11-12$). A water molecule protonates the pyridine nitrogen and the pyrrole is deprotonated to another water molecule from the solvent leading to the formation of phototautomer **4-T**. Therefore, in the appropriate pH range phototautomer **4-T** was detected by LFP by its characteristic strong transient absorption with a maximum at 390 nm. Phototautomer **4-T** in near-neutral solution ($pH 8-10$) decays through uni- and bimolecular reactions, as indicated by the

1
2
3 dependence of decay on the laser pulse energy. As anticipated the formation and decay of **4-T** is
4
5 pH dependent and susceptible to deuterium isotope effect. The decay kinetics for **4-T** is probably
6
7 governed by general and specific acid and base catalysis. Such acid/base catalysis was
8
9 demonstrated for example in the hydration reactions of quinone methides,⁷³ or keto-enol
10
11 tautomerisations.^{74,75}
12
13

14
15 The driving force for the formation of phototautomer **4-T** was investigated by molecular
16
17 modeling. The energy for the vertical excitation of **4** to S_1 calculated at the B3LYP/6-311G level
18
19 of theory in the gas phase is 366 kJmol^{-1} (Table S1 in the SI), which perfectly matches the
20
21 experimentally observed absorption of **4** in CH_3CN ($\lambda_{\text{max}} = 327 \text{ nm}$, 365.8 kJmol^{-1}). The S_1 state
22
23 of **4** has a significant CT character, as evidenced by the fluoro-solvatochromic properties and the
24
25 calculated dipole moment (Table S3 in th SI). The CT character is the driving force for ESPT to
26
27 occur. The calculated energy of the S_1 state of **4-T** in the gas phase is higher, 390 kJmol^{-1} (Fig.
28
29 S3 and S4, and Tables S2, and S5 in the SI). However, we have no evidence that **4-T** is formed
30
31 in the excited state. Its formation may involve double ESPT by solvent molecules in an adiabatic
32
33 exergonic reaction, or passing through a conical intersection, leading to **4-T** in S_0 .
34
35
36
37
38
39
40
41
42
43
44
45
46
47
48
49
50
51
52
53
54
55
56
57
58
59
60

Scheme 8. Energy diagram for **4** and **4-T**.

Kinetics for **4-T** formation could not be studied since the tautomerization takes place within the laser pulse (10 ns). Protonation and deprotonation may take place simultaneously, or sequentially. Furthermore, we have no experimental evidence if the tautomerization involves a H_2O -relay mechanism as was suggested for 7-azaindoles¹⁸ and 7-hydroxyquinoline.^{19,20,21,22,23} Phototautomer **4-T** is 145 kJ mol^{-1} higher in energy than **4**, which sets the stage for the tautomerization in the ground state back to the starting molecule, taking place between 200 ns to 4 μs , depending on the pH of the solution.

In an aprotic solvent, excitation of **4** to S_1 leads to parallel reactions, where homolytic cleavage of the pyrrole N-H forms radical **10**, and photoionization of **4** forms radical-cation **9**. The radical-cation is acidic and deprotonates to pyrrolyl radical **10**. Similarly, excitation of 4H^+ in an aprotic solvent ultimately leads to the formation of **10**, involving homolytic cleavage of the pyrrole N-H bond to form radical-cation **9'** followed by deprotonation to **10**. These processes probably take place also in aqueous solution, but with a quantum efficiency significantly lower

1
2
3 than for the phototautomerization. Therefore, radical **10** can be detected by LFP after the decay
4
5 of **4-T**. However, the minor pathways involving homolytic cleavage leading to radicals **10**
6
7 become dominant in acidic aqueous solutions at $\text{pH} < \text{p}K_a^*$ for the deprotonation of pyrrole in S_1 .
8
9 Positively charged **4H⁺** formed a stable host-guest complex with CB[7] with a β_{11} value of $(1.0 \pm$
10
11 $0.2) \times 10^5 \text{ M}^{-1}$. Stabilization of the positive charge in the complex increased the $\text{p}K_a$ value of the
12
13 pyridine nitrogen, and presumably decreased the pyrrole acidity. Therefore, within the cavity of
14
15 CB[7] the pyrrole NH in **4H⁺** cannot deprotonate to give phototautomer **4-T**. Instead, the
16
17 competitive homolytic N-H bond cleavage ultimately leading to the formation of pyrrolyl radical
18
19 **10** becomes the dominant photochemical process (as presented in Scheme 6). Consequently, the
20
21 complexation with CB[7] fundamentally changes the reactivity of the molecule so that instead of
22
23 proton transfer it undergoes homolytic cleavage.
24
25
26
27
28

29 The results presented herein have demonstrated the operation of H₂O-mediated long-range ESPT
30
31 in terphenyl derivatives **2-4**. The ability to control this process by pH and complexation with
32
33 CB[7] is of particular importance. It implicates the use of the investigated systems for the
34
35 rational design of functional molecules with potential applications in different research fields
36
37 such as photochemical switching, drug delivery vehicles, logic gates, sensing, operation of
38
39 proton pumps in biological systems, where the photochemistry of these terphenyl derivatives can
40
41 be modulated by changes in pH or complexation to supramolecular hosts.
42
43
44
45
46
47

48 **Conclusion**

49 Pyrrolylphenylpyridine terphenyl derivatives **2-4** were synthesized and their photophysical
50
51 properties and photochemical reactivity in phototautomerization reactions was investigated. On
52
53 excitation to S_1 in polar protic solvents, **2-4** populate CT states leading to the enhanced basicity
54
55
56
57
58
59
60

1
2
3 of pyridine and enhanced acidity of pyrrole. The difference in acid-base properties enables
4
5 excited state proton transfer (ESPT) giving rise to phototautomers **2-T**, **3-T** and **4-T**.
6
7 Phototautomers **2-T** and **4-T** were detected by LFP by their characteristic strong transient
8
9 absorption at 380-450 nm, whereas zwitterionic **3-T** formed from the *meta*-derivative could not
10
11 be detected probably due to its short lifetime. The decays for **2-T** and **4-T** were non-exponential
12
13 due to competing mono- and bimolecular reactions. The estimated lifetimes for **2-T** and **4-T** are
14
15 1.5 μs , and 4 μs at pH 9 and a shortening of the lifetime of **4-T** was observed at higher pH
16
17 values. The pyridinium salt **4H⁺** forms a stable complex with CB[7] with 1:1 stoichiometry (β_{11}
18
19 of $(1.0 \pm 0.2) \times 10^5 \text{ M}^{-1}$). The complexation increases the $\text{p}K_{\text{a}}$ of **4** and changes its photochemical
20
21 reactivity. Due to decreased acidity of the pyrrole phototautomerization in the inclusion complex,
22
23 the formation of the tautomer does not take place but homolytic cleavage of the pyrrole NH leads
24
25 to the formation of radicals, as is also observed in non-protic polar solvents.
26
27
28
29
30
31
32
33
34
35

36 Experimental section

37 General

38
39 ¹H and ¹³C NMR spectra were recorded at 300, or 600 MHz at rt using TMS as a reference and
40
41 chemical shifts were reported in ppm. Melting points were determined using a Mikroheiztisch
42
43 apparatus and were not corrected. IR spectra were recorded on a spectrophotometer in KBr and
44
45 the characteristic peak values were given in cm^{-1} . HRMS were obtained on a MALDI TOF/TOF
46
47 instrument. Irradiation experiments were performed in a reactor equipped with 16 lamps with the
48
49 output at 350 nm or a reactor equipped with 8 lamps. During the irradiations, the irradiated
50
51 solutions were continuously purged with Ar and cooled by a tap-water finger-condenser.
52
53
54
55
56
57
58
59
60

1
2
3 Solvents for irradiations were of HPLC purity. Chemicals were purchased from the usual
4 commercial sources and were used as received. Solvents for chromatographic separations were
5 used as they are delivered from supplier (p.a. grade) or purified by distillation (CH₂Cl₂).
6
7
8
9
10 Calculations were performed using Gaussian 03 software.⁷⁶
11
12
13

14 15 **2-(4-Bromophenyl)pyridine (6)**^{44,45} 16

17 In a refluxing solution of 2-bromopyridine (960 mg, 6.0 mmol) and
18 tetrakis(triphenylphosphine)palladium(0) (80 mg, 0.07 mmol) in dioxane (20 mL), a solution of
19 *p*-bromophenylboronic acid (**5**, 660 mg, 3.3 mmol) in aqueous K₂CO₃ (20 mL, 2 M) was added
20 dropwise during 8 h under nitrogen. After additional 8 h of reflux, the reaction was quenched
21 with H₂O (50 mL) and extracted with CH₂Cl₂ (3×30 mL). The extracts were dried over
22 anhydrous MgSO₄, filtered and the solvent was removed on a rotational evaporator. The crude
23 compound was purified using silica column chromatography with CH₂Cl₂/EtOAc (1:1), which
24 afforded pure compound (405 mg, 29 %).
25
26
27
28
29
30
31
32
33
34
35

36 Colorless oil; ¹H NMR (CDCl₃, 300 MHz) δ/ppm 8.68 (ddd, 1H, *J* = 1.0, 1.6, 4.8 Hz), 7.87 (d,
37 2H, *J* = 8.6 Hz), 7.75 (ddd, 1H, *J* = 1.6, 8.0, 7.0 Hz), 7.69 (ddd, 1H, *J* = 1.0, 1.6, 8.0 Hz), 7.59 (d,
38 2H, *J* = 8.6 Hz), 7.24 (ddd, 1H, *J* = 1.6, 4.8, 6.2 Hz).
39
40
41
42
43
44

45 46 **3-(4-bromophenyl)pyridine (7)**^{49,50} 47

48 A solution of 3-pyridineboronic acid (200 mg, 1.62 mmol), *p*-dibromobenzene (766 mg, 1.63
49 mmol) and tetrakis(triphenylphosphine)palladium(0) (40 mg, 0.035 mmol) in dioxane (20 mL)
50 and aqueous K₂CO₃ (20 mL, 2M) was refluxed for 16 h under nitrogen. The reaction mixture
51 was quenched with H₂O (50 mL) and extracted with CH₂Cl₂ (3×30 mL). The organic layer was
52
53
54
55
56
57
58
59
60

dried over magnesium sulfate, filtered and evaporated. The extracts were dried over anhydrous MgSO_4 , filtered and the solvent was removed on a rotational evaporator. The crude compound was purified using silica column chromatography with $\text{CH}_2\text{Cl}_2/\text{EtOAc}$ (1:1), which afforded the pure compound (290 mg, 76 %).

Colorless oil; ^1H NMR (CDCl_3 , 300 MHz) δ /ppm 8.81 (d, 1H, $J = 2.2$ Hz), 8.61 (dd, 1H, $J = 1.6$, 4.8 Hz), 7.83 (ddd, 1H, $J = 2.2$, 4.0, 8.0 Hz), 7.61 (d, 2H, $J = 8.4$ Hz), 7.44 (d, 2H, $J = 8.4$ Hz), 7.36 (dd, 1H, $J = 4.9$, 8.0 Hz).

4-(4-bromophenyl)pyridine (**8**)⁴⁸

Solution of dry pyridine (0.8 mL, 10 mmol) in dry ether (100 mL) was cooled to 0 °C under nitrogen and trifluoromethylsulfonic anhydride (1.68 mL, 10 mmol) was added dropwise with vigorous stirring. The resulting mixture was stirred for 30 min and then cooled to -78 °C. In another flask *p*-dibromobenzene (2.36 g, 10 mmol) was dissolved in dry ether (15 mL) under nitrogen and cooled to -78 °C. A solution of *n*-butyllithium (2.5 M, 5.2 mL) was added dropwise. The resulting organolithium reagent was cannulated to the flask containing pyridine triflate with vigorous stirring during 10 min, and the mixture was left to warm to rt. The reaction was quenched with aqueous NaOH (100 mL, w = 5 %) and stirred for 10 min. The organic layer was separated, dried over sodium carbonate and filtered. Evaporation of the solvent afforded crude 4-(4-bromophenyl)-1-(trifluoromethylsulfonyl)-1,4-dihydropyridine that was purified on a silica column with hexane/ CH_2Cl_2 (1:1). The isolated compound was stirred for 12 h in a mixture of dioxane (20 mL) and aqueous NaOH (20 mL, w = 20 %). After dilution with H_2O the compound was extracted with CH_2Cl_2 (3×30 mL). The extracts were dried over anhydrous MgSO_4 , filtered

1
2
3 and the solvent was removed on a rotational evaporator to afford the pure compound (585 mg, 25
4
5
6 %).

7
8 Pale yellow crystals; ¹H NMR (CDCl₃, 300 MHz) δ/ppm 8.66 (d, 2H, *J* = 6.3 Hz), 7.61 (d, 2H, *J*
9
10 = 8.6 Hz), 7.50 (d, 2H, *J* = 8.6 Hz), 7.46 (d, 2H, *J* = 6.3 Hz).
11
12
13

14 15 **General procedure for the Suzuki coupling and the Boc-deprotection**

16
17 In a refluxing mixture of bromophenylpyridine (1.9 mmol),
18
19 tetrakis(triphenylphosphine)palladium(0) (0.095 mmol) and cesium carbonate (3.78 mmol) in
20
21 toluene (40 mL) under argon, a solution of *N*-Boc-2-pyrrolboronic acid (1.9 mmol) was added
22
23 dropwise during 8 h. After addition the resulting solution was refluxed for additional 2 h and
24
25 then stirred at rt overnight. The reaction was quenched with H₂O (50 mL), the organic layer was
26
27 separated and the aqueous layer extracted with CH₂Cl₂ (3×30 mL). The combined organic
28
29 extracts were dried over anhydrous MgSO₄, filtered and the solvent was removed on a rotational
30
31 evaporator. To the resulting crude compound, a solution of sodium methoxide prepared from
32
33 sodium (400 mg, 17.3 mmol) and methanol (100 mL) was added and the mixture was refluxed
34
35 under nitrogen for 3 h. The solvent was evaporated, H₂O (50 mL) was added and extraction with
36
37 CH₂Cl₂ (3×30 mL) was carried out. The combined organic extracts were washed with brine,
38
39 dried over anhydrous MgSO₄, filtered and the solvent was removed on a rotational evaporator.
40
41 The crude compound was purified using silica column chromatography with EtOAc/CH₂Cl₂
42
43 (1:4) as eluent.
44
45
46
47
48
49
50
51
52

53 **2-(4-(1H-pyrrol-2-yl)phenyl)pyridine (2)**⁴⁸
54
55
56
57
58
59
60

1
2
3 In a reaction of 2-(4-bromophenyl)pyridine (**6**, 250 mg, 1.1 mmol),
4
5 tetrakis(triphenylphosphine)palladium(0) (90 mg, 0.08 mmol) and cesium carbonate (750 mg,
6
7 2.3 mmol) *N*-Boc-2-pyrrolboronic acid (240 mg, 1.0 mmol) the crude compound was obtained.
8
9 After refluxing with sodium methoxide prepared with sodium (380 mg, 16 mmol) and column
10
11 chromatography the pure compound was obtained (60 mg, 26 %).
12
13

14
15 Colorless crystals, ¹H NMR (C₆D₆, 300 MHz) δ/ppm 8.62 (d, 1H, *J* = 4.7 Hz), 8.17 (d, 2H, *J* =
16
17 8.5 Hz), 7.41 (br s, 1H), 7.38 (d, 1H, *J* = 7.9 Hz), 7.29 (d, 2H, *J* = 8.5 Hz), 7.14 (dd, 1H, *J* = 1.5,
18
19 7.9 Hz), 6.67 (ddd, 1H, *J* = 1.2, 4.7, 7.9 Hz), 6.64-6.61 (m, 1H), 6.44-6.41 (m, 1H), 6.37-6.32
20
21 (m, 1H); ¹³C NMR (C₆D₆, 75 MHz) δ/ppm 157.2 (s), 150.0 (d), 137.2 (s), 136.3 (d), 133.9 (s),
22
23 131.7 (s), 127.7 (d), 124.2 (d), 121.8 (d), 119.7 (d), 119.4 (d), 110.5 (d), 107.2 (d).
24
25
26
27
28

29 **3-(4-(1H-pyrrol-2-yl)phenyl)pyridine (3)**

30
31 In a reaction of 3-(4-bromophenyl)pyridine (**7**, 280 mg, 1.2 mmol),
32
33 tetrakis(triphenylphosphine)palladium(0) (70 mg, 0.06 mmol), cesium carbonate (780 mg, 2.4
34
35 mmol) and *N*-Boc-2-pyrrolboronic acid (250 mg, 1.0 mmol) crude compound was obtained.
36
37 After refluxing with sodium methoxide prepared with sodium (380 mg, 16 mmol) and column
38
39 chromatography the pure compound was obtained (50 mg, 23 %).
40
41
42

43
44 Colorless crystals; mp = 174-176 °C; IR (cm⁻¹, KBr) 3402, 3135, 1607, 1480, 1416, 1106, 843,
45
46 792, 728; ¹H NMR (C₆D₆, 300 MHz) δ/ppm 9.00 (d, 1H, *J* = 2.1 Hz), 8.54 (dd, 1H, *J* = 1.5, 4.7
47
48 Hz), 7.58-7.44 (m, 1H), 7.41 (d, 1H, *J* = 8.4 Hz), 7.27 (d, 2H, *J* = 8.2 Hz), 7.19 (d, 2H, *J* = 8.2
49
50 Hz), 6.80 (dd, 1H, *J* = 4.7, 7.6 Hz), 6.65-6.59 (m, 1H), 6.48-6.43 (m, 1H), 6.39-6.33 (m, 1H); ¹³C
51
52 NMR (C₆D₆, 150 MHz) δ/ppm 148.8 (d), 148.7 (d), 136.3 (s), 135.6 (d), 133.5 (s), 133.1 (s),
53
54
55
56
57
58
59
60

1
2
3
4
5
6
7
8
9
10
11
12
13
14
15
16
17
18
19
20
21
22
23
24
25
26
27
28
29
30
31
32
33
34
35
36
37
38
39
40
41
42
43
44
45
46
47
48
49
50
51
52
53
54
55
56
57
58
59
60

131.5 (s), 124.6 (d), 123.5 (d), 119.5 (d), 110.6 (d), 107.1 (d); HRMS (MALDI-TOF): m/z $[M + e]^-$ calcd for $(C_{15}H_{12}N_2)^-$ 220.0995; found 220.0990.

4-(4-(1H-pyrrol-2-yl)phenyl)pyridine (4)

In a reaction of 4-(4-bromophenyl)pyridine (**8**, 75 mg, 0.34 mmol), tetrakis(triphenylphosphine)palladium(0) (40 mg, 0.034 mmol), cesium carbonate (220 mg, 0.68 mmol) and *N*-Boc-2-pyrrolboronic acid (72 mg, 0.30 mmol) crude compound was obtained. After preparative TLC on silica and ethyl-acetate/dichloromethane (1:4) as eluent, the compound was refluxed with sodium methoxide prepared with sodium (380 mg, 16 mmol) and column chromatography the pure compound was obtained (52 mg, 74 %).

Pale yellow crystals; mp = 170-172 °C; IR (cm^{-1} , KBr) 3122, 1593, 1488, 1413, 1283, 1222, 1116, 992, 818, 726; 1H NMR ($CDCl_3$, 300 MHz) δ/ppm 8.65 (d, 2H, $J = 6.2$ Hz), 8.62-8.53 (m, 1H), 7.66 (d, 2H, $J = 8.4$ Hz), 7.58 (d, 2H, $J = 8.4$ Hz), 7.52 (d, 2H, $J = 6.2$ Hz), 6.94-6.90 (m, 1H), 6.64-6.60 (m, 1H), 6.36-6.31 (m, 1H); ^{13}C NMR ($CDCl_3$, 75 MHz) δ/ppm 150.2 (d), 147.6 (s), 135.3 (s), 133.4 (s), 131.1 (s), 127.4 (d), 124.2 (d), 121.1 (d), 119.4 (d), 110.4 (d), 106.8 (d); HRMS (MALDI-TOF): m/z $[M + H]^+$ calcd for $(C_{15}H_{13}N_2)^+$ 221.1073; found 221.1074.

By adding an ethereal solution of HCl to the solution of **4** in dry ether, the hydrochloride salt **4H⁺** precipitated quantitatively. The salt was filtered and washed with ether affording yellow-green crystals; mp = 186-188 °C; IR (cm^{-1} , KBr) 3415, 3250, 1633, 1601, 1481, 1297, 1125, 802; 1H NMR ($DMSO-d_6$, 300 MHz) δ/ppm 11.56 (s, 1H), 8.85 (d, 2H, $J = 6.0$ Hz), 8.33 (d, 2H, $J = 6.0$ Hz), 8.05 (d, 2H, $J = 8.2$ Hz), 7.85 (d, 2H, $J = 8.2$ Hz), 7.00-6.94 (m, 1H), 6.79-6.72 (m, 1H), 6.23-6.15 (m, 1H); ^{13}C NMR ($DMSO-d_6$, 75 MHz) δ/ppm 143.0 (s), 135.9 (s), 130.5 (s), 129.9 (s), 128.4 (d), 123.9 (d), 122.4 (d), 121.1 (d), 109.7 (d), 107.9 (d).

Steady-State and Time-Resolved Fluorescence Measurements

Steady-state measurements were performed with a QM-2 fluorimeter (PTI). The samples were dissolved in cyclohexane, CH₃CN, or CH₃CN-H₂O (1:1) and the concentrations were adjusted to absorbances of less than 0.1 at the excitation wavelengths of 310, 320, or 330 nm. Solutions were purged with nitrogen for 30 min prior to analysis. Measurements were performed at 20 °C. Fluorescence quantum yields were determined by comparison of the integral of the emission bands with the one of quinine sulfate in 0.05 M aqueous H₂SO₄ ($\Phi_f = 0.53$).⁵² For **4H**⁺, acridine yellow in CH₃OH was used as a reference ($\Phi_f = 0.57$).⁵³ Typically, three absorption traces were recorded (and averaged) and three fluorescence emission traces were collected by exciting the sample at three different wavelengths. Three quantum yields were calculated (eq. S1 in the SI) and the mean value was reported.

Fluorescence decays, collected over 1023 time channels, were obtained on an Edinburgh Instruments OB920 single photon counter using light emitting diodes for excitation (excitation wavelength 335 nm, or 310 nm for cyclohexane solutions). The instrument response functions (using LUDOX scatterer) were recorded at the same wavelengths as the excitation wavelength and had a half width of ≈ 0.2 ns. Emission decays for samples in CH₃CN solutions were recorded at 410, 430, and 450 nm, while in cyclohexane solutions the decays were measured at 360, 370 and 390 nm. The counts in the peak channel were 3×10^3 . For aqueous solutions, the decays were collected at 450 and 470 nm until they reached 1×10^3 counts in the peak channel. The time increment per channel was 0.01753 ns. Obtained histograms were fit as sums of exponentials using global Gaussian-weighted non-linear least-squares fitting based on Marquardt-Levenberg

1
2
3 minimization implemented in the Fast software package from Edinburgh Instruments. The fitting
4
5 parameters (decay times and pre-exponential factors) were determined by minimizing the global
6
7 reduced chi-square χ^2 and graphical methods were used to judge the quality of the fit that
8
9 included plots of the weighted residuals vs. channel number.
10
11
12
13

14 15 **Determination of pK_a and pK_a^* for 2-4**

16 17 **UV-vis titration**

18
19 A stock solution of $4H^+$ (1.35 mg) was prepared in CH_3CN (20 mL). The stock solution (20 μL)
20
21 was diluted to 25 mL with H_2O ($[4H^+] = 5.3 \times 10^{-6}$ M) and this dilute solution was titrated with a
22
23 diluted solution of NaOH until pH 9 was reached. The pH of this latter solution was decreased to
24
25 3.0 with the addition of a diluted solution of HCl. The pH was measured with a pH-meter and
26
27 UV-vis spectra were recorded. The measurements were performed at 25 °C. The resulting UV-
28
29 vis spectra were processed by multivariate nonlinear regression analysis using the SPECFIT
30
31 program. In the analysis a surface was fit that is defined by all UV-vis spectra from 242 to 486
32
33 nm at different pH values.
34
35
36
37

38
39 Alternatively, a stock solution of $4H^+$ (1.30 mg or 3.42 mg) in CH_3CN (10 mL or 25 mL) was
40
41 prepared and was diluted with H_2O to achieve a $4H^+$ concentration of 1.05×10^{-5} M. A series of
42
43 solutions was prepared by mixing the diluted $4H^+$ solution in a 1:1 ratio with a solution of
44
45 phosphate buffer of the appropriate pH (obtained by mixing H_3PO_4 , NaH_2PO_4 and Na_2HPO_4).
46
47 The total concentrations of compound and buffer after dilution was 5.3×10^{-6} M, and 0.05 M,
48
49 respectively.
50
51
52

53 For measurements in the presence of citrate buffer, a stock solution was prepared by dissolving
54
55 $4H^+$ (3.25 mg), **3** (2.77 mg) or **2** (2.91 mg) in CH_3CN (25 mL), and the solutions were diluted
56
57
58
59
60

1
2
3 with H₂O to reach a concentration of 1.06×10^{-4} M. A series of solutions was prepared by
4
5 mixing the diluted **4H⁺**, **3**, or **2** solution in a 1:1 ratio with citrate buffer of the appropriate pH.
6
7
8 The total concentrations of compounds and buffer after dilution was 5.3×10^{-5} M, and 0.05 M,
9
10 respectively.
11

12 13 14 15 **Fluorescence titration**

16
17 The solutions of **2**, **3** and **4H⁺** (5.3×10^{-6} M) in the presence of citrate buffer (0.05 M) were
18
19 prepared as described for the UV-vis studies. The pH was measured by a pH-meter and
20
21 fluorescence spectra at 25 °C were recorded on a spectrometer with slits set for a bandwidth of
22
23 10 or 20 nm for the excitation and emission monochromator. The resulting fluorescence spectra
24
25 were processed by multivariate nonlinear regression analysis using the SPECFIT program. In the
26
27 analysis, the surface was fit defined by all fluorescence spectra in the wavelength region from
28
29 410 to 680 nm.
30
31
32

33 34 35 36 **Determination of the equilibrium constant between 4H⁺ and CB[7]**

37
38 A stock solution of **4H⁺** (545 μM) was prepared in CH₃CN. A solution of citrate buffer (47 mM)
39
40 was prepared by dissolving citric acid monohydrate (0.7122 g) and trisodium citrate dihydrate
41
42 (0.3807 g) in H₂O (100 mL). The buffer had a pH of 3.5. A solution of CB[7] (597 μM) in H₂O
43
44 was prepared, to which no NaCl was added. The citrate buffer was used to prepare the solution
45
46 of **4H⁺** and had a Na⁺ cation concentration of 39 mM. In the titration experiment, **4H⁺** was
47
48 diluted with citrate buffer to reach a final concentration of 5 μM. The variations in the
49
50 absorbance of **4H⁺** with additions of CB[7] were measured with a UV-vis spectrophotometer.
51
52
53 Absorption spectra for blank solutions containing all chemicals except **4H⁺** were subtracted from
54
55
56
57

1
2
3 the spectra. Corrected absorbance values were used to determine the overall equilibrium binding
4 constant for the complexation between 4H^+ and CB[7]. The fitting of the binding isotherm was
5 performed using the Scientist 3 software (see SI). A 1:1 binding model was used to fit the data.
6
7
8
9
10 During the titration, 4H^+ solution was diluted by 5% and this dilution was taken into account
11 during the fitting.
12
13

14 15 16 17 18 **Determination of the pK_a for 4H^+ complexed with CB[7]**

19
20 A stock solution of 4H^+ (1.27 mg) in CH_3CN (10 mL) with a concentration of 4.95×10^{-4} M was
21 prepared. A stock solution of CB[7] (1.0×10^{-3} M) was prepared by dissolving CB[7] (75.41 mg,
22 79% purity determined by titration)⁷⁷ in aqueous solution of NaCl (50 mL of 0.1 M NaCl). A
23 series of solutions was prepared by adding 40 μL 4H^+ to 1.96 mL of the CB[7] solution and then
24 mixing with 2.0 mL of phosphate buffer of the appropriate pH (obtained by mixing NaH_2PO_4
25 and Na_2HPO_4). The total concentration of 4H^+ , CB[7] and the buffer after dilution were $4.95 \times$
26 10^{-6} M, 5.02×10^{-4} M, and 0.05 M, respectively. The pH was measured by a pH-meter and the
27 UV-vis spectra were recorded. The spectra were corrected by subtracting the spectrum of the
28 solution containing CB[7] (1.96 mL), CH_3CN (40 μL), and the phosphate buffer at pH 6.11 (2
29 mL). The measurements were performed at 25 °C. The resulting UV-vis spectra were processed
30 by multivariate nonlinear regression analysis using the SPECFIT program. In the analysis the
31 surface was fit defined by 18 UV-vis spectra in the wavelength region from 242 to 486 nm.
32
33
34
35
36
37
38
39
40
41
42
43
44
45
46
47
48
49
50

51 **Laser Flash Photolysis (LFP)**

52
53 All LFP studies on a system previously described⁷⁸ employed as an excitation source a Quanta-
54 Ray Lab 130–4 pulsed Nd:YAG laser at 355 nm from Spectra Physics (<20 mJ per pulse), with a
55
56
57
58
59
60

1
2
3 pulse width of 10 ns. Static cells (7 mm × 7 mm) were used and the solutions were purged with
4
5 nitrogen or oxygen for 20 min prior to performing the measurements. Absorbances at 355 nm
6
7 were ~ 0.3-0.4.
8
9

10 For LFP experiments conducted at different pH values, the pH of the aqueous solution was
11
12 measured by a pH-meter, adjusted with H₂SO₄, NaOH or citrate buffer (*c* = 0.05 M), and then
13
14 this aqueous solution was mixed with the CH₃CN solution of **4**. The pH of the resulting CH₃CN-
15
16 H₂O (1:1) solution was not measured.
17
18
19

20 21 22 **Acknowledgement**

23
24 These materials are based on work financed by the Croatian Foundation for Science (HRZZ), the
25
26 Natural Sciences and Engineering Research Council (NSERC) of Canada and the University of
27
28 Victoria.
29
30
31

32
33
34 **Supporting information contains:** computational results, UV-vis and fluorescence spectra, pH
35
36 titration data for **2-4**, titration data for **4** and **4H⁺** with CB[7], LFP data and ¹H and ¹³C NMR
37
38 spectra of new compounds. This material is available free of charge via the Internet at
39
40 <http://pubs.acs.org>.
41
42
43
44

45 46 **References:**

47
48
49 ¹ Hydrogen-transfer reactions, Hynes, J.T.; Klinman, J.P.; Limbach, H.-H.; Schowen, R.L., Eds.;
50 Wiley-VCH: Weinheim, 2007.

51
52 ² Kwon, J.I.; Park, S.Y., *Adv. Mater.* **2011**, *23*, 3615-3642.

53
54
55 ³ Ireland, J.F.; Wyatt, P.A.H., *Adv. Phys. Org. Chem.* **1976**, *12*, 131-221.
56
57

- 1
2
3
4
5
6
7
8
9
10
11
12
13
14
15
16
17
18
19
20
21
22
23
24
25
26
27
28
29
30
31
32
33
34
35
36
37
38
39
40
41
42
43
44
45
46
47
48
49
50
51
52
53
54
55
56
57
58
59
60
-
- ⁴ Arnaut, L.G.; Formosinho, S.J., *J. Photochem. Photobiol. A: Chem.* **1993**, *75*, 1-20.
- ⁵ Klöpffer, W., *Adv. Photochem.* **1977**, *10*, 311-358.
- ⁶ Formosinho, S.J.; Arnaut, L.G., *J. Photochem. Photobiol. A: Chem.* **1993**, *75*, 21-48.
- ⁷ Ormson, S.M.; Brown, R.G., *Prog. React. Kinet.* **1994**, *19*, 45-91.
- ⁸ Le Gourrierec, D.; Ormson, S.M.; Brown, R.G., *Prog. React. Kinet.* **1994**, *19*, 211-275.
- ⁹ Kasha, M., *J. Chem. Soc. Faraday Trans. 2*, **1986**, *82*, 2379-2392.
- ¹⁰ Lill, M.A.; Helms, V., *Proc. Nat. Acad. Sci.* **2002**, *99*, 2778-2781.
- ¹¹ Faxén, K.; Gilderson, G.; Ädelroth, P.; Brzezinski, P., *Nature* **2005**, *437*, 286-289.
- ¹² Schäfer, L.V.; Groenhof, G.; Klingen, A.R.; Ullmann, G.L.; Boggio-Pasqua, M.; Robb, M.A.; Grubmüller, H., *Angew. Chem. Int. Ed.* **2007**, *46*, 530-536.
- ¹³ Sobolewski, A. J.; Domcke, W., *ChemPhysChem* **2006**, *7*, 561-564.
- ¹⁴ Meyer, T.J.; Huynh, M. H. V.; Thorp, H. H., *Angew. Chem. Int. Ed.* **2007**, *46*, 5284-5304.
- ¹⁵ Hosler, J.P.; Ferguson-Miller, S.; Mills, D. A., *Annu. Rev. Biochem.* **2006**, *75*, 165-187.
- ¹⁶ Royant, A.; Edman, K.; Ursby, T.; Pebay-Peyroula, E.; Landau, E.M.; Neutze, R., *Nature* **2000**, *406*, 645-648.
- ¹⁷ Mathias, G.; Marx, D., *Proc. Nat. Acad. Sci.* **2007**, *104*, 6980-6985.
- ¹⁸ Kwon, O.-H.; Lee, Y.-S.; Park, H.J.; Kim, Y.; Jang, D.-J., *Angew. Chem. Int. Ed.* **2004**, *43*, 5792-5796.
- ¹⁹ Kohtani, S.; Tagami, A.; Nakagaki, R., *Chem. Phys. Lett.* **2000**, *316*, 88-93.
- ²⁰ Park, H.-J.; Kwon, O.-H.; Ah, C.S.; Jang, D.-J., *J. Chem. Phys. B* **2005**, *109*, 3938-3943.
- ²¹ Kwon, O.-H.; Lee, Y.-S.; Yoo, B.K.; Jang, D.-J., *Angew. Chem. Int. Ed.* **2006**, *45*, 415-419.
- ²² Park, S.-Y.; Lee, Y.-S.; Kwon, O.-H.; Jang, D.-J., *Chem. Commun.* **2009**, 926-928.
- ²³ Park, S.-Y.; Jang, D.-J., *J. Am. Chem. Soc.* **2010**, *132*, 297-302.
- ²⁴ Smirnov, A.V.; English, D.S.; Rich, R.L.; Lane, J.; Teyton, L.; Schwabacher, A.W.; Luo, S.; Thornburg, R.W.; Petrich, J.W., *J. Chem. Phys. B* **1997**, *101*, 2758-2769.

- 1
2
3
4
5 25 Mukherjee, T. K.; Panda, D.; Datta, A., *J. Phys. Chem. B* **2005**, *109*, 18895-18901.
6
7 26 Mukherjee, T. K.; Datta, A., *J. Phys. Chem. B* **2006**, *110*, 2611-2617.
8
9 27 Kyrychenko, A.; Wu, F.; Thummel, R. P.; Waluk, J.; Ladokhin, A. S., *J. Phys. Chem. B* **2010**,
10 *114*, 13574-13578.
11
12 28 Kyrychenko, A.; Herbich, J.; Waluk, J. in *Tautomerism Methods and Theories*. Antonov L.
13 (Ed.) Wiley-VCH, Weinheim: 2014. pp 49.
14
15 29 Herbich, J.; Rettig, W.; Waluk, J., *Chem. Phys. Lett.* **1992**, *195*, 556-562.
16
17 30 Herbich, J.; Hung, C.-Y.; Thummel, R.P.; Waluk, J., *J. Am. Chem. Soc.* **1996**, *118*, 3508-3518.
18
19 31 Kijak, M.; Zielińska, A.; Chamchoumis, C.; Herbich, J.; Thummel, R.P.; Waluk, J., *Chem.*
20 *Phys. Lett.* **2004**, *400*, 279-285.
21
22 32 Petkova, I.; Mudadu, M.S.; Singh, A.; Thummel, R.P.; van Stokkum, I.H.M.; Buma, W.J.;
23 Waluk, J., *J. Phys. Chem. A* **2007**, *111*, 11400-11409.
24
25 33 Nosenko, Y.; Wiosna-Sałyga, G.; Kunitski, M.; Petkova, I.; Singh, A.; Buma, W.J.; Thummel,
26 R.P.; Brutschy, B.; Waluk, J., *Angew. Chem. Int. Ed.* **2008**, *47*, 6037-6040.
27
28 34 Kyrychenko, A.; Herbich, J.; Thummel, R.P.; Waluk, J., *J. Am. Chem. Soc.* **2000**, *122*, 2818-
29 2827.
30
31 35 Wiosna, G.; Petkova, I.; Mudadu, M.S.; Thummel, R.P.; Waluk, J., *Chem. Phys. Lett.* **2004**,
32 *400*, 379-383.
33
34 36 Vetohkina, V.; Kijak, M.; Wiosna-Sałyga, G.; Thummel, R.P.; Herbich, J.; Waluk,
35 *Photochem. Photobiol. Sci.*, **2010**, *9*, 923-930.
36
37 37 Assaf, K. I.; Nau, W. M., *Chem. Soc. Rev.* **2015**, *44*, 394-418.
38
39 38 Pavari, G.; Reany, O.; Keinan, O., *Isr. J. Chem.* **2011**, *51*, 646-663.
40
41 39 Macartney, D.H.; *Isr. J. Chem.* **2011**, *51*, 600-615.
42
43 40 Walker, S.; Oun, R.; McInnes, F.J.; Wheate, N.J., *Isr. J. Chem.* **2011**, *51*, 616-624.
44
45 41 Day, A.I.; Collins, J.G., In: *Supramolecular Chemistry: From Molecules to Nanomaterials*,
46 Steed, J. W.; Gale, P. A. Eds, John Wiley & Sons, 2012.
47
48 42 Lagona, J.; Mukhopadhyay, P.; Chakrabarti, S.; Isaacs, L., *Angew. Chem. Int. Ed.* **2005**, *44*,
49 4844-4870.
50
51
52
53
54
55
56
57
58
59
60

- 1
2
3
4
5
6
7
8
9
10
11
12
13
14
15
16
17
18
19
20
21
22
23
24
25
26
27
28
29
30
31
32
33
34
35
36
37
38
39
40
41
42
43
44
45
46
47
48
49
50
51
52
53
54
55
56
57
58
59
60
- ⁴³ Masson, E.; Ling, X.; Joseph, R.; Kyeremeh-Mensah, L.; Lu, X., *RSC Advances* **2012**, *2*, 1213-1247.
- ⁴⁴ Butterworth, E. C.; Heilbron, I. M.; Hey, D. H. *J. Chem. Soc.* **1940**, 355-358.
- ⁴⁵ Hey, D. H.; Stirling, C. J. M.; Gareth H. W., *J. Chem. Soc.* **1955**, 3963-3969.
- ⁴⁶ Martina, S.; Enkelmann, V.; Wegner, G.; Schlüter, A.-D., *Synthesis* **1991**, 613-615.
- ⁴⁷ Alešković, M.; Basarić, N.; Mlinarić-Majerski, K., *J. Heterocycl. Chem.* **2011**, *48*, 1329-1335.
- ⁴⁸ Lucchesini, F. *Tetrahedron* **1992**, *48*, 9951-9966.
- ⁴⁹ Choi-Sledeski, Y. M.; McGarry, D. G.; Green, D. M.; Mason, H.J.; Becker, M. R.; Davis, R. S.; Ewing, W. R.; Dankulich, W. P.; Manetta, V. E.; Morris, R. L.; Spada, A. P.; Cheney, D. L.; Brown, K. D.; Colussi, D. J.; Chu, V.; Heran, C. L.; Morgan, S. R.; Bentley, R. G.; Leadley, R. J.; Maignan, S.; Guilloteau, J.-P.; Dunwiddie, C. T.; Pauls, H. W., *J. Med. Chem.* **1999**, *42*, 3572-3587.
- ⁵⁰ Wakabayashi, S.; Sugihara, Y.; Takakura, K.; Murata, S.; Tomioka, H.; Ohnishi, S.; Tatsumi, K. *J. Org. Chem.* **1999**, *64*, 6999-7008.
- ⁵¹ Toscano, R. A.; Hernández-Galindo, M. C.; García-Mellado, R. R. O.; Portilla, F. R.; Amábile-Cuevas, C.; Álvarez-Tolenado, C., *Chem. Pharm. Bull.* **1997**, *45*, 957-961.
- ⁵² Montalti, M.; Credi, A.; Prodi, L.; Gandolfi, M.T., In *Handbook of Photochemistry*; CRC Taylor and Francis: Boca Raton, 2006.
- ⁵³ Olmsted, J., *J. Phys. Chem.* **1979**, *83*, 2581-2584.
- ⁵⁴ Grampp, H.; Maeder, M.; Meyer, C.J.; Zuberbühler, A.D. *Talanta* **1985**, *32*, 95-101.
- ⁵⁵ Grampp, H.; Maeder, M.; Meyer, C.J.; Zuberbühler, A.D. *Talanta* **1985**, *32*, 257-264.
- ⁵⁶ Grampp, H.; Maeder, M.; Meyer, C.J.; Zuberbühler, A.D. *Talanta* **1985**, *32*, 1133-1139.
- ⁵⁷ Joule, J.A.; Mills, K., *Heterocyclic Chemistry*, Blackwell Publishing, Oxford: 2000.
- ⁵⁸ Tang, H.; Fuentealba, D.; Ho Ko, Y.; Selvapalam, N.; Kim, K.; Bohne, C., *J. Am. Chem. Soc.* **2011**, *133*, 20623-20633.
- ⁵⁹ Mohanty, J.; Bhasikuttan, A.C.; Nau, W.M.; Pal, H., *J. Phys. Chem. B* **2006**, *110*, 5132-5138.;
- ⁶⁰ Koner, A.L.; Ghosh, I.; Saleh, N.; Nau, W.M., *Can. J. Chem.* **2011**, *89*, 139-147.

- 1
2
3
4
5
6
7
8
9
10
11
12
13
14
15
16
17
18
19
20
21
22
23
24
25
26
27
28
29
30
31
32
33
34
35
36
37
38
39
40
41
42
43
44
45
46
47
48
49
50
51
52
53
54
55
56
57
58
59
60
- ⁶¹ Shaikh, M.; Dutta Choudhury, S.; Mothany, J.; Bhasikuttan, A.C.; Nau, W.M.; Pal, H., *Chem. Eur. J.* **2009**, *15*, 12362-12370.
- ⁶² Pischel, U.; Uzunova, V.D.; Remón, P.; Nau, W.M., *Chem. Commun.* **2010**, *46*, 2635-2637.
- ⁶³ Shaikh, M.; Mohanty, J.; Bhasikuttan, A.C.; Uzunova, V.D.; Nau, W.M.; Pal, H., *Chem. Commun.* **2008**, *44*, 3681-3683.
- ⁶⁴ Saleh, N.; Koner, A.L.; Nau, W.M., *Angew. Chem. Int. Ed.* **2008**, *47*, 5398-5401.
- ⁶⁵ Parente Carvalho, C.; Uzunova, V.D.; Da Silva, J.P.; Nau, W.M.; Pischel, U., *Chem. Commun.* **2011**, *47*, 8793-8795.
- ⁶⁶ Basarić, N.; Franco-Cea, A.; Alešković, M.; Mlinarić-Majerski, K.; Wan, P., *Photochem. Photobiol. Sci.* **2010**, *9*, 779-790.
- ⁶⁷ Bent, D.V.; Hayon, E., *J. Am. Chem. Soc.*, **1975**, *97*, 2612-2619.
- ⁶⁸ Moorthy, P.N.; Hayon, E.; *J. Phys. Chem.*, **1974**, *78*, 2615-2620.
- ⁶⁹ Fang, X.; Jin, F.; Jin, H.; von Sonntag, C., *J. Chem. Soc. Perkin 2* **1998**, 259-263.
- ⁷⁰ Basarić, N.; Wan, P., *Photochem. Photobiol. Sci.* **2006**, *5*, 656-664.
- ⁷¹ Hansen, P.E. in *Tautomerism Methods and Theories*. Antonov L. (Ed.) Wiley-VCH, Weinheim: 2014. pp143.
- ⁷² Basarić, N.; Cindro, N.; Bobinac, D.; Uzelac, L.; Mlinarić-Majerski, K.; Kralj, M.; Wan, P., *Photochem. Photobiol. Sci.* **2012**, *11*, 381-396.
- ⁷³ Chiang, Y.; Kresge, A.J.; Zhu, Y., *J. Am. Chem. Soc.* **2000**, *122*, 9854-9855.
- ⁷⁴ Wirz, J., *Pure Appl. Chem.* **1998**, *70*, 2221-2232.
- ⁷⁵ A. P. Pelliccioli, P. Šebej, J. Wirz, *Photochem. Photobiol. Sci.* **2012**, *11*, 967-971.
- ⁷⁶ Gaussian 03, Rev E. 01, Frisch, M. J.; Trucks, G. W.; Schlegel, H. B.; Scuseria, G. E.; Robb, M. A.; Cheeseman, J. R.; Montgomery, Jr., J. A.; Vreven, T.; Kudin, K. N.; Burant, J. C.; Millam, J. M.; Iyengar, S. S.; Tomasi, J.; Barone, V.; Mennucci, B.; Cossi, M.; Scalmani, G.; Rega, N.; Petersson, G. A.; Nakatsuji, H.; Hada, M.; Ehara, M.; Toyota, K.; Fukuda, R.; Hasegawa, J.; Ishida, M.; Nakajima, T.; Honda, Y.; Kitao, O.; Nakai, H.; Klene, M.; Li, X.; Knox, J. E.; Hratchian, H. P.; Cross, J. B.; Adamo, C.; Jaramillo, J.; Gomperts, R.; Stratmann, R. E.; Yazyev, O.; Austin, A. J.; Cammi, R.; Pomelli, C.; Ochterski, J. W.; Ayala, P. Y.; Morokuma, K.; Voth, G. A.; Salvador, P.; Dannenberg, J. J.; Zakrzewski, V. G.; Dapprich, S.;

1
2
3
4
5 Daniels, A. D.; Strain, M. C.; Farkas, O.; Malick, D. K.; Rabuck, A. D.; Raghavachari, K.;
6 Foresman, J. B.; Ortiz, J. V.; Cui, Q.; Baboul, A. G.; Clifford, S.; Cioslowski, J.; Stefanov, B. B.;
7 Liu, G.; Liashenko, A.; Piskorz, P.; Komaromi, I.; Martin, R. L.; Fox, D. J.; Keith, T.; Al-
8 Laham, M. A.; Peng, C. Y.; Nanayakkara, A.; Challacombe, M.; Gill, P. M. W.; Johnson, B.;
9 Chen, W.; Wong, M. W.; Gonzalez, C.; and Pople, J. A.; Gaussian, Inc., Pittsburgh PA, 2003.
10
11

12 ⁷⁷ Yi, S.; Kaifer, A. E., *J. Org. Chem.* **2011**, *76*, 10275-10278.
13

14 ⁷⁸ Liao, Y.; Bohne, C. *J. Phys. Chem.*, **1996**, *100*, 734-743.
15
16
17
18
19
20
21
22
23
24
25
26
27
28
29
30
31
32
33
34
35
36
37
38
39
40
41
42
43
44
45
46
47
48
49
50
51
52
53
54
55
56
57
58
59
60